

# The crossing of the historical centre of Rome by the new underground Line C: a study of soil structure-interaction for historical buildings

A. Burghignoli, L. Callisto & S. Rampello

*Università degli Studi di Roma La Sapienza, Roma, Italy*

F.M. Soccodato

*Università degli Studi di Cagliari, Cagliari, Italy*

G.M.B. Viggiani

*Università degli Studi di Roma Tor Vergata, Roma, Italy*

**ABSTRACT:** This work deals with the soil structure-interaction problems posed by the construction of the third line of Roma underground (Line C), which, in its central stretch, crosses the historical centre of the city with significant interferences with the archaeological and monumental heritage. The paper describes the methodological approach developed to evaluate the effects of tunnelling on the existing monuments and historical buildings, starting from a careful geotechnical and structural characterisation and including the development of reliable geotechnical and structural models. Experts in several disciplines were committed to this multidisciplinary work, ranging from geologists to geotechnical and structural engineers, archaeologists, and professionals working in the field of conservation and restoration of works of art and monuments. The study of the interaction between the construction activities and the built environment was carried out following procedures of increasing level of complexity, from green field analyses, in which the stiffness of the existing buildings was neglected, to full soil-structure interaction analyses, performed in both two- and three-dimensional conditions, accounting for the stiffness of existing buildings and considering possible long-term effects. The paper illustrates the main aspects of this procedure, using the example case studies of the Basilica di Massenzio and of the building of the Amministrazione Doria Pamphili.

## 1 INTRODUCTION

The growing demand for public and sustainable transport in heavily urbanised areas requires the construction of an increasing number of underground infrastructures. In Italian cities, the use of collective transport is still not fully developed: for example, in Roma public transport covers less than 30% of motorised mobility, compared to 67.7% in Barcelona, 63.3% in Paris, and 47.7% in London. The many constraints and technical challenges associated to the construction of underground infrastructures often lead to high costs and long completion times. This is particularly true in Italy, where many towns are characterised by a high density of population, significant archaeological heritage, and the presence of masonry structures of historical and monumental value, which are particularly sensitive to subsidence induced by excavation. It is therefore often necessary to adopt complex control systems of the excavation process in order to limit the deformations, to devise intense monitoring schemes, and, where necessary, to implement techniques for the protection of the structures affected by the excavation, and these activities result in larger construction costs.

At present, the existing underground network in Rome consists of only two lines, Line A and Line B, intersecting at Termini Central Railway Station. Line B was built during the 1930s by cut-and-cover techniques whereas the bored tunnels of Line A date back only a few decades, as the line was constructed in the 1970s. A northward extension of Line B, or Line B1, has just been completed. The third line of Roma underground, or Line C, will run northwest to southeast across the city centre, for a total length of more than 25 km and 30 stations. The Municipality of

Roma approved its preliminary design in October 2002; the tender for detailed design and construction of the line was finally awarded in February 2006, with a value of about 3 billion Euros.

The construction of the south-eastern part of the line is currently under way, while the central stretch of the line, running through the historical centre, from S. Giovanni to Castel S. Angelo, is at a stage of advanced design. This part of the line is particularly challenging because of the geotechnical characteristics of the soil, and the need to minimise the effects on the historical and monumental heritage.

The Authors of this paper had the opportunity to be involved in the project from the very early stages of design, when the Municipality of Roma required the contribution of the University to examine the complex problem of the interaction between the historical and monumental built environment and the construction of the line along Contract T3, from S. Giovanni to Piazza Venezia. A large research team, involving geotechnical and structural engineers from several universities, was set up to respond to the concern of the Superintendence for the protection of the cultural heritage that the construction of this infrastructure could affect adversely the existing monuments. The interaction studies, developed by the team over two years, laid the foundations of a methodological approach that eventually percolated into the contractual requirements included in the tender for the design and construction of Contract T3, between S. Giovanni and Piazza Venezia and Contract T2, between Piazza Venezia and Clodio/Mazzini.

As a matter of fact, the tender included an obligation for the General Contractor to establish an independent technical structure, consisting of a Scientific and Technical Steering Committee (STSC) and several Working Groups (WG), that would undertake detailed studies of the interaction between the line and the monuments that required specific attention. The same technical structure was also to identify the most appropriate and possibly reversible measures for the protection of those monuments that, according to the results of the studies, required intervention.

This was a work of multidisciplinary nature of such complexity as to require the commitment of many scholars, experts in disciplines ranging from geology to geotechnical and structural engineering, archaeology, and conservation and restoration of works of art and monuments.

## 2 THE CITY ALONG THE TRACK OF LINE C

### 2.1 *The visible city*

This section explores the visible city along the route of Contracts T3 and T2 of Line C of Roma underground, starting from S. Giovanni Station, where the line intersects the existing Line A and Contract T3 starts (Fig. 2.1).



Figure 2.1 – Line C of Roma Underground: Contracts T2 and T3

Emerging at surface from the station and following the Aurelian Walls along Via Sannio, the route encounters Porta Asinaria (Figure 2.2a), one of the Roman gates in the Aurelian Walls. Following the historic market of via Sannio, the route reaches the first station of Contract T3, at Amba Aradam-Ipponio; under-passing the Aurelian Walls at Porta Metronia, it gets to the Churches of Santo Stefano Rotondo and Santa Maria in Domnica (Figures 2.2 c and d).

Now in the Rione Celio, the line makes a wide curve to the right to get to the Military Hospital and then another wide curve to the left that takes it to the Coliseum, or Anfiteatro Flavio, (Figure 2.2e), skirted along its north side, to make its way towards Colle Oppio and reaching the second station of the contract, at Fori Imperiali. The route continues along Via dei Fori Imperiali towards Piazza Venezia, in the heart of Roma, passing close to a number of outstanding buildings, including the Basilica di Massenzio (Figure 2.2f) the Colonnacce of the Foro di Traiano, the Foro di Augusto, and the Mercato di Traiano.



(a)



(b)



(c)



(d)



(e)



(f)

Figure 2.2 – The monuments along Contract T3



From Venezia Station, the route of now Contract T2 continues in the historic centre of the city along the busy Via del Plebiscito, where many important buildings are potentially affected by the line, such as the Church of S. Marco and Palazzo Venezia (Fig. 2.3a), Palazzo Grazioli, Palazzo Altieri, and the Church of S. Andrea della Valle (Fig. 2.3b). The route arrives at Largo di Torre Argentina, where there are some of the most ancient monuments of republican Rome, and then, after skirting the Church of Gesù, continues along Corso Vittorio Emanuele, close to a number of historical buildings and churches, including Palazzo Vidoni Caffarelli, Palazzo Braschi, Palazzo Massimo alle Colonne (Fig. 2.3e), Palazzo della Cancelleria (Fig. 2.3 c), Palazzo Sforza Cesarini, and the Churches of Sant'Andrea della Valle and of San Lorenzo in Damaso. The second station of Contract T2 is at Chiesa Nuova, just in front of the Chiesa Nuova and the Convento dei Filippini (Fig. 2.3d). Before leaving the baroque bend of the river, the route passes very close to the Antica Zecca (Ancient Mint) (Fig. 2.3f) and then continues across the Tiber river between Via della Conciliazione and Castel Sant'Angelo.



(a)



(b)



(c)



(d)



(e)



(f)

Figure 2.3 – The monuments along Contract T2

## 2.2 The underground city and the geological setting

In its underground crossing of the historic centre, the route of Line C encounters all the main geological features of the site where the city of Roma developed over the centuries; to a certain extent it is these geological features that justify the age and diversity of the surface built environment.

The establishment of the city of Rome was favoured by several auspicious environmental factors, such as the proximity of a navigable river, the presence of abundant spring water, and the nearby existence of quarries for construction materials. For these reasons, the expansion of the city was influenced by the geological factors that have determined its development and that it is useful to recall briefly here.

In the Pliocene and Pleistocene, the sea submerged the area of Roma (see Fig. 2.4a). The so-called Unit of Monte Vaticano, which represents the basic formation of the subsoil of Rome, was formed in this period; it consists of a deposit of stiff overconsolidated grey-blue clay, nearly 800 m thick.

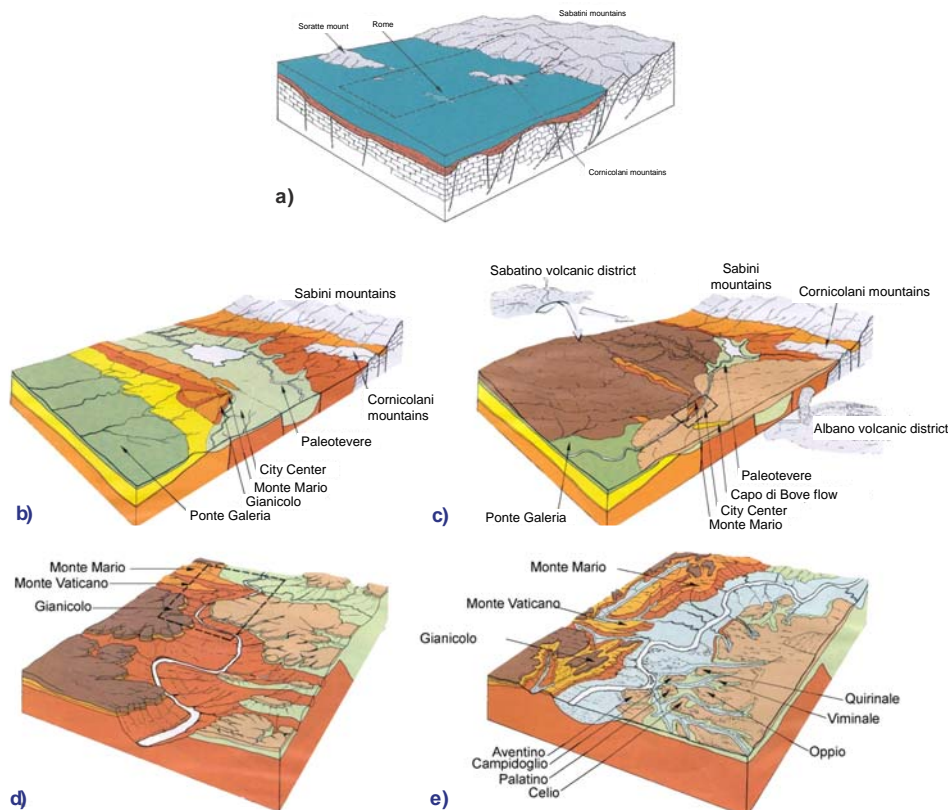


Figure 2.4 – Geological evolution of the Roman area from Pliocene to Olocene, from Parotto (1990)

In the Middle Pleistocene, the uplift of the region and the consequent regression of the sea involved several relocations of the course of the Tiber River, which moved first to the southwest and then to the south. This period is associated to the deposition of a sequence of continental fluvial-marshy deposits consisting of gravel, sand and clay (Fig. 2.4b).

The volcanic districts of the Colli Albani and Colli Sabatini formed in the Middle-Upper Pleistocene; the associated eruptions and pyroclastic flows changed the course of the Tiber River, moving it to the north, in its present position (Fig. 2.4c).

Due to the regression of the sea that accompanied the last ice age, the Tiber River cut steadily and deeply into the volcanic and pre-volcanic formations, reaching the Pliocene clays (Fig. 2.4d); the surviving slabs of volcanic debris anticipate the topography of the present hills of Roma.

During the Holocene, the raising sea level caused progressive filling of the Tiber Valley, which separates the area of Monte Mario – Gianicolo to the west, from the relict volcanic slabs, or the "seven hills", to the east (Fig. 2.4e).

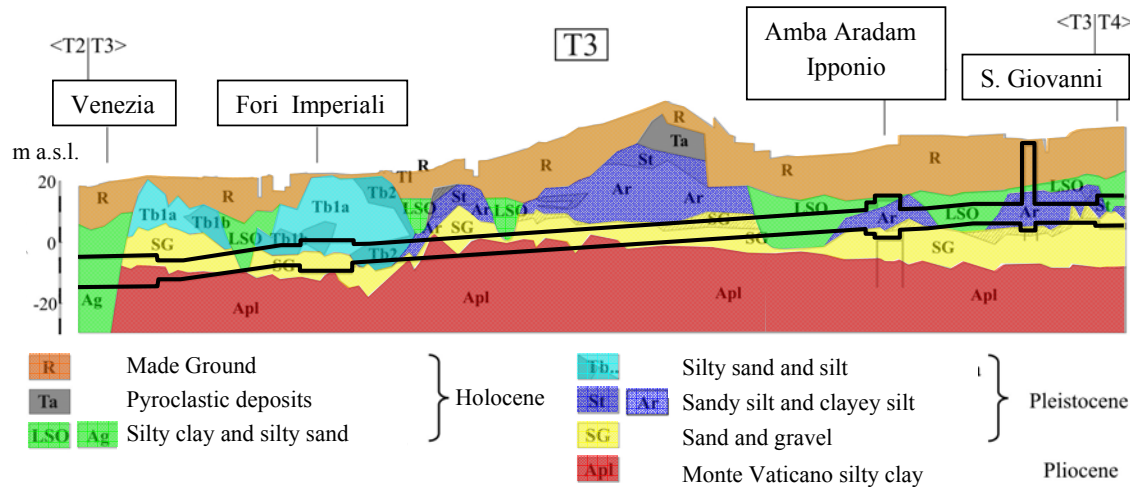


Figure 2.5 - Geological profile along Contract T3

In the stretch under examination, Line C runs from S. Giovanni towards Piazza Venezia at an elevation of about 9.5 m above sea level (a.s.l.) or a depth of about 25 m below ground level (b.g.l.) (Fig. 2.5). The elevation of the track gradually reduces to about 5 m a.s.l. near Piazza Celimontana, corresponding to a depth of 45 m b.g.l., and then increases again to about 0.25 m a.s.l. at Fori Imperiali Station; from this point the line deepens towards Venezia Station, at an absolute elevation of -10 m a.s.l.

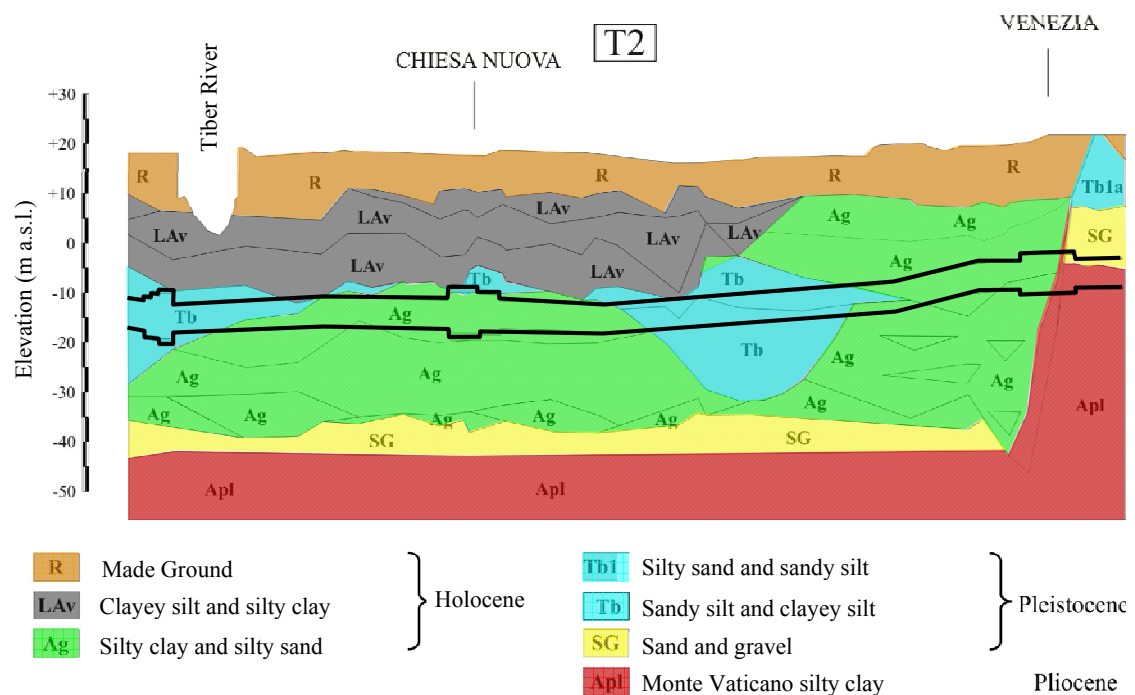


Figure 2.6 - Geological profile along Contract T2

In the first part of Contract T3, up to Largo dell'Amba-Aradam, the tunnels run mainly into fine-grained Pleistocene and Holocene soils. After a short passage through the overlying Pleistocene sandy-gravel, the tunnels enter the base Pliocene clay, to emerge again into the overlying formations of sands and gravels, and sands, silts and clays of the Pleistocene, near the Coliseum.



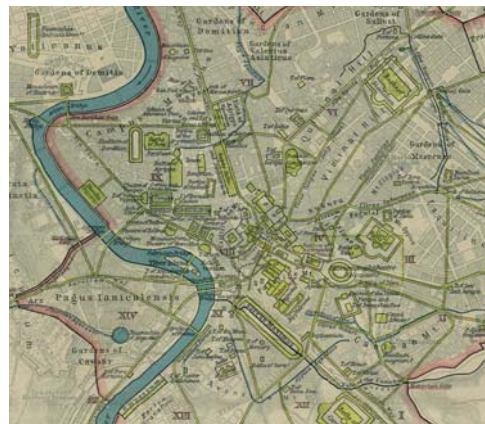
At Piazza Venezia there is an abrupt change of the geological environment, as the tunnels enter the Tiber Valley with its Holocene fine and medium grained soils; from here until the end of Contract T3 the tunnels are contained in these type of soils (Fig. 2.6).

The pore water pressure distribution along the central stretch of the line is almost hydrostatic, with local small downward gradients; the ground water table is between 10 and 15 m b.g.l. along Contract T3 and between 6 and 8 m b.g.l. along Contract T2.

Between the visible city at surface and the underlying geological environment there are other buried cities, often destroyed and flattened, testifying to the long history of Roma. Figure 2.7 shows the maps of Rome in 40 BC and 350 AD, while Figure 2.8 shows the expansion of the city in 1840, before the breakthrough of the urban fabric in the Baroque bend of the Tiber river and in the area of the Roman Forum.



(a)



(b)

Fig. 2.7 – Maps of Rome in (a) Republican and (b) Imperial ages



Fig. 2.8 – Map of Rome in 1841

The long history of demolitions and reconstructions taking place over the centuries modified gradually the aspect of the city and, at same time, changed significantly its altimetry, as demonstrated by the relevant thickness of made ground, which, in the area under examination, ranges between 7 and 11 m. The layer of made ground contains the remnants of the ancient city and has an immense archaeological value; any excavation carried out in the historical centre of Roma, for whatever purposes, is bound to raise the interest of the Superintendence for Archaeological Heritage. This requires that preliminary investigations are carried out and authorizations obtained before undertaking the works, often rendering any estimate of their duration and overall costs extremely uncertain.

### 2.3 Tunnelling method

Construction of Line C includes excavation of two running tunnels with a diameter of 6.7 m, using Earth Pressure Balance (EPB) Tunnel Boring Machines (TBM).

The essence of an EPB machine for tunnelling in soft ground is provision of substantial support to the excavated face at all times, thereby controlling ground movements. Face support is provided by the cutterhead, powered by a drive motor, contained within the circular steel skin of the TBM. The soil, excavated by the rotating cutter wheel, passes into the excavation chamber immediately behind the cutterhead. The excavated material is removed from the excavation chamber by an auger conveyor (cochlea).

The screw conveyor plays an important role in the excavation process. As the machine advances through the ground, the excavated soil enters the pressurised head chamber. The soil is extracted from the head chamber and flows along the screw conveyor to the discharge outlet, where it is discharged at atmospheric pressure onto a conveyor belt. The rotational speed of the screw and the opening of the upper auger conveyor driver influence the soil flow rate and pressure gradient along the screw conveyor. Controlling the rate of soil discharge and the pressure gradient along the screw conveyor regulates the head chamber pressure supporting the tunnel face. If the machine advances steadily, a reduction in the screw conveyor extraction rate will cause an increase in pressure in the excavation chamber; correspondingly, an increase in extraction rate will result in a reduction in chamber pressure.

The factors influencing the chamber pressure during excavation are complex but the details of the screw conveyor operation are of particular relevance. It is important that the extraction of the soil is well controlled, synchronised with the speed of excavation, and that the soil mixture is converted to a low shear strength paste by suitable soil conditioning. This is achieved by injecting conditioning agents, most commonly foams or polymers, into the cutterhead to mix with the soil during the excavation process. The parameters that have to be selected for the soil conditioning comprise the type of product (water, bentonite, polymer, foam or any combination of these) as well as their quantities.

The tunnel is lined with reinforced concrete segments, which are positioned under atmospheric pressure by means of an erector arm in the rear area of the shield. As the tail skin leaves the tunnel lining, grout is injected under pressure to fill the annular void between the extrados of the segmental lining and the excavated ground. Tail skin seals prevent the grout from entering the TBM. Appropriate control of the excavation parameters and timely and effective tail skin grouting with mixtures of low permeability are the determining factors to obtain very low values of volume loss. With this type of TBMs the volume loss is generally lower than 1%.

## 3 EFFECTS OF TUNNELLING AT SURFACE

### 3.1 Subsidence

Urban tunnels are typically shallow and, as such, interact with the built environment.

In green field conditions, *i.e.*, in the absence of structures, the settlement trough induced by tunnelling has a characteristic shape (Fig. 3.1). The available field evidence indicates that the surface settlement trough may be described by a Gaussian distribution curve in a section transversal to the tunnel axis, at sufficient distance from the face to assume plane strain conditions, and by a cumulative probability function in the longitudinal direction (Peck, 1969, O'Reilly and New, 1982).

The transverse surface settlement trough can be written in the form:

$$w = w_{\max} \cdot \exp\left(\frac{-y^2}{2 \cdot i^2}\right) \quad (1)$$

where  $w$  is the vertical displacement a distance  $y$  from the tunnel axis,  $w_{\max}$  is the maximum vertical displacement, controlling the magnitude of the subsidence, and  $i$  is the distance of the point of inflection of the Gaussian curve from the tunnel axis, defining the width of the settlement trough ( $\cong 6i$ ).



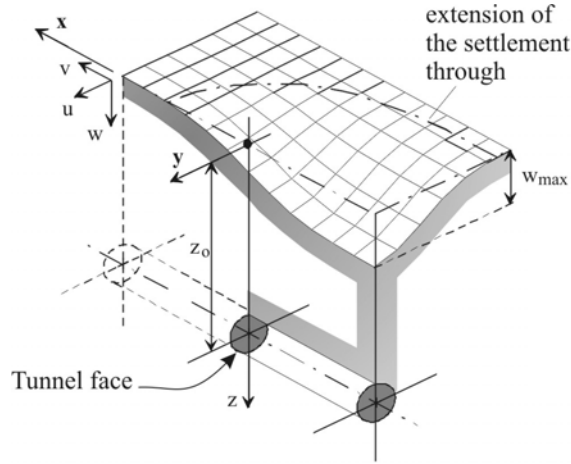


Fig. 3.1 – Subsidence trough in greenfield conditions

The volume of the surface settlement trough per unit length of advancement,  $V_S$ , can be obtained by integration of the Gaussian curve:

$$V_S = \sqrt{2\pi} \cdot i \cdot w_{\max} \quad (2)$$

In saturated fine-grained soils and undrained conditions, the volume of the settlement trough at surface is equal to the over-excavated volume at the tunnel. In coarse-grained soils this is not the case, as the volume of the settlement trough at surface may be less than the over excavated volume, due to dilatancy of dense sand on shearing. Whatever the soil type, it is convenient to define the volume loss,  $V_L$ , as the (percentage) ratio of the volume of the surface settlement trough and the excavated nominal volume of tunnel, *i.e.*, for a circular tunnel of diameter  $D$ :

$$V_L = \frac{4V_S}{\pi D^2} \quad (3)$$

In the present study, values of the volume loss between 0.5% (contractual requirement) and 1.0% (worst case scenario) were used. Combining equations (2) and (3), it is possible to express  $w_{\max}$  as:

$$w_{\max} = \frac{V_L \cdot \pi D^2 / 4}{\sqrt{2\pi} \cdot i} \quad (4)$$

For relatively deep tunnels, *i.e.*, tunnels with a cover at least equal to one diameter, the value of  $i$  at surface is proportional to the depth of the tunnel axis,  $z_0$  (O'Reilly e New, 1982):

$$i_0 = K \cdot z_0 \quad (5)$$

through a width parameter,  $K$ , that depends on the type of soil between tunnel crown and surface, and takes values in the range 0.2 - 0.3 for sands above the water table, 0.4 - 0.5 for stiff clays, and 0.6 - 0.7 for soft clays (Ribacchi, 1993). In the present study, values of  $K = 0.4$  to 0.5 were assumed at ground surface.

For ground movements at depth it is typically assumed (O'Reilly & New, 1982; Grant & Taylor, 2000) that the shape of the transversal settlement trough is still Gaussian so that eq. (1) can be used to compute the profiles of vertical displacements at any depth  $z$  below ground surface, once  $w_{\max}$  and the variation of  $i = K(z) \cdot (z_0 - z)$  with  $z$  are defined.

Several relationships to evaluate  $i$  at depth have been proposed in the literature, such as those by Mair *et al.* (1993), for stiff clays:

$$i(z) = 0.5z_0 - 0.325z \quad (6)$$

or by Moh *et al.* (1993), for coarser grained soils:

$$i(z) = bD \left( \frac{z_0 - z}{D} \right)^m \quad (7)$$

in which  $b$  and  $m$  are parameters that depend on the characteristics of the soil. The present study adopted the expression by Moh *et al.* (1996) with values of the exponent  $m = 0.6$  that is in between the values of 0.4 and 0.8 recommended for silty-sands and silty-clays, respectively. Parameter  $b$  was obtained from the value of  $i$  at surface:

$$i(z=0) = i_0 = b \cdot D \cdot \left( \frac{z_0}{D} \right)^m \quad (8)$$

or:

$$i(z) = i_0 \cdot \left( \frac{z_0 - z}{z_0} \right)^m \quad (9)$$

To evaluate the horizontal components of displacements it was assumed that the vectors of displacement in the plane orthogonal to the tunnel axis point towards the centre of the tunnel (O'Reilly & New, 1982), and, therefore, the horizontal displacements,  $u$ , can be computed from the vertical displacements as:

$$u(y, z) = \frac{y}{z_0 - z} \cdot w(y, z) \quad (10)$$

In the longitudinal direction, the vertical displacements may be computed as (O'Reilly & New, 1982, Attewell & Woodman, 1982):

$$w(x, y, z) = w_{\max} \cdot \exp\left(\frac{-y^2}{2 \cdot i(z)^2}\right) \cdot F\left(\frac{x}{i(z)}\right) \quad (11)$$

Where  $F(x)$  is the a cumulative probability function:

$$F(x) = \int_{-\infty}^x \frac{1}{\sqrt{2\pi}} \cdot \exp\left(\frac{-t^2}{2}\right) \cdot dt \quad (12)$$

The displacement field described so far is relative to the short term, resulting from the progress of excavation and the installation of the lining. For tunnels excavated in fine-grained soils, settlements can increase with time due to the change in the hydraulic conditions at the tunnel internal boundary, where pore pressures are equal to zero. Reviewing the long-term settlements measured in clays after tunnel construction, Mair and Taylor (1997) concluded that the major factors influencing their development are the initial pore water pressure distribution, the excess pore water pressure generated by tunnel construction, the compressibility of the clay and, most significantly, the ratio of the permeability of the tunnel lining to that of the soil. Mair (2008) discussed example case studies, showing that the tunnel lining should be regarded as a porous material.

Wongsaroy (2005) identified the key factors affecting possible long-term effects and introduced two dimensionless variables:

$$DS = \frac{w_{\max} - w_{\max, \text{imp}}}{w_{\max, \text{per}} - w_{\max, \text{imp}}} \quad (13)$$

$$RP = \frac{k_l}{k_s} \frac{z_0 - 0.5D}{t} \quad (14)$$

in which  $w_{\max}$ ,  $w_{\max,imp}$ , and  $w_{\max,per}$  are the actual maximum long-term settlement and the maximum long term settlements for a totally impermeable and totally permeable lining,  $k_l$  and  $k_s$  the coefficients of permeability of the lining and the soil, and  $t$  the thickness of the lining.

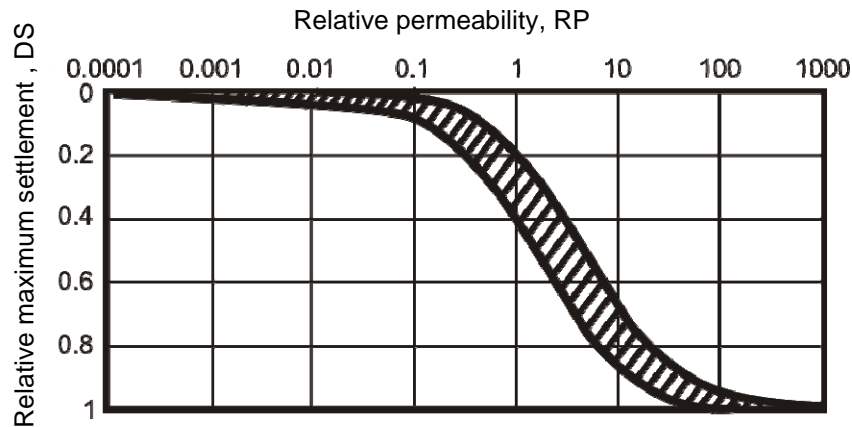


Fig. 3.2 – Effects of soil-lining relative permeability on the long-term maximum settlement (Mair, 2008)

The results of the parametric study by Wongsaroy (2005), shown in Figure 3.2, indicate that the lining can be considered as perfectly impermeable if the relative permeability of the lining to the soil is less than 0.1 and wholly permeable if the relative permeability is larger than 100, which can be used to orient design of lining and clogging injections.

Despite the fact that the long-term settlements are generally larger than in the short term, their effects on the existing structures are generally limited because they tend to increase the width of the settlement profile thus reducing differential settlements, curvatures and distortions.

### 3.2 Interaction with structures at surface

The displacement field generated by the excavation of the tunnel propagates to the surface, thus interacting with the existing buildings located within the settlement trough.

The buildings that are closer to the tunnel axis tend to assume a deformed configuration with an upward concavity (*sagging*), while the buildings that are far from the tunnel axis, beyond the point of inflection of the settlement profile, tend to assume a deformed configuration with a downward concavity (*hogging*). The presence of structures modifies the shape of the settlement trough, typically reducing distortions and curvatures, to a greater or lesser extent depending on their stiffness. If the values of curvature exceed given thresholds, the structures will experience damage of varying severity, all the way from simple aesthetic to severe structural damage. In general, buildings suffer more from the hogging than from the sagging mode of deformation (see Figure 3.3). This due to the restraining effect produced by the ground and by the foundations in the lower part of the structure, while in the hogging mode, which is generally missing in the upper parts of the structure.

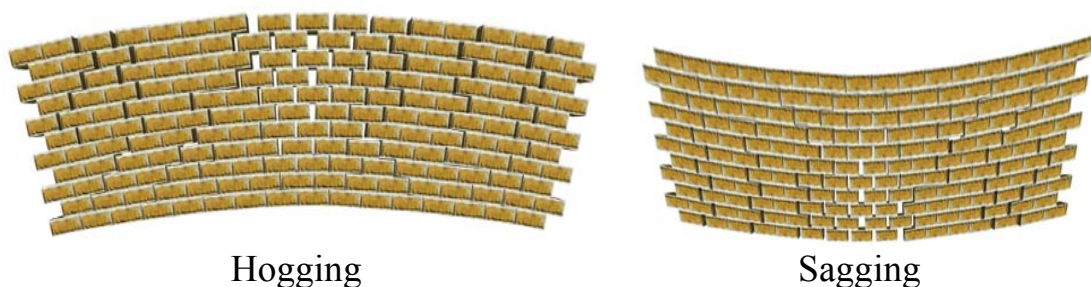


Fig. 3.3 – Hogging and sagging in masonry walls



Older or ancient buildings are often already affected by damage of various origin, mainly connected to self weight, manifesting with existing crack patterns; new damage can arise as intensification of existing cracks but may also affect parts of the building that had not been previously affected by damage due to self weight or other causes. All these factors must be taken into account in the assessment of expected damage to old structures.

#### 4 EXPECTED DAMAGE

Developing a rational and completely objective evaluation of the risk of damage to historical structures due to tunnelling and deep excavations is not an easy task. The wealth of historical, artistic and monumental buildings potentially affected by the construction of Line C of Roma underground made it necessary to reconsider the concept of damage and its identification and classification. Following the approach by Burland *et al.* (1977), in this study risk is associated with a potential degree of damage, so that the judgment on a low or high level of risk is reduced to the evaluation of a low or high degree of damage. This justifies the establishment of a classification of damage, illustrated in the following section, connecting its severity to representative indicators.

##### 4.1 Classification of damage

Burland *et al.* (1977) proposed a classification of damage to masonry buildings. The classification is based on the ease of repair and provides information on the visible effects of damage, such as crack widths.

Tab. 4.1 – Damage classification, after Burland *et al.* (1977).

Category of damage	Normal degree of severity	Description of typical damage (ease of repair in bold type) Note: Crack width is only one factor in assessing category of damage and should not be used on its own as a direct measure of it
0	Negligible	Hairline cracks less than about 0.1 mm wide
1	Very slight	<b>Fine cracks that are easily treated during normal decoration.</b> Damage generally restricted to internal wall finishes. Close inspection may reveal some cracks in external brickwork or masonry. Typical cracks widths up to 1 mm
2	Slight	<b>Cracks easily filled. Redecoration probably required. Recurrent cracks can be masked by suitable linings.</b> Cracks may be visible externally and <b>some repointing may be required to ensure weather-tightness.</b> Doors and windows stick slightly. Typical crack widths up to 5 mm.
3	Moderate	<b>The cracks requires some opening up and can be patched by a mason. Repointing of external brickwork and possibly a small amount of brickwork to be replaced.</b> Doors and windows sticking. Service pipes may fracture. Weather tightness often impaired. Typical crack widths are 5-15 mm or several > 3 mm
4	Severe	<b>Extensive repair work involving breaking-out and replacing sections of walls, especially over doors and windows.</b> Windows and door frames distorted, floor sloping noticeably. Walls leaning or bulging noticeably, some loss of bearing in beams. Service pipes disrupted. Typical cracks widths are 15-25 mm but also depends on the number of cracks.
5	Very severe	<b>This requires a major repair job involving partial or complete rebuilding.</b> Beams lose bearing, walls lean badly and require shoring. Windows broken with distortion. Danger of instability. Typical crack widths are greater than 25 mm, but depends on the number of cracks.

The classification in Table 4.I identifies six categories of damage of increasing severity, from negligible to very severe, which can be grouped into three broader classes: damage affecting appearance or visual aesthetics (categories 0, 1, and 2), function (categories 3 and 4), and stability (category 5). It is probably worth to recall that different causes, such as thermal effects or seasonal oscillations of the groundwater table, may result in damage up to category 2.

Evaluating the crack pattern induced by tunnelling or the evolution of the pre-existing crack pattern is a very complex task, because of the difficulty of modelling adequately the structural behaviour of masonry. Assuming that cracking of the walls results mainly from tensile strains, Burland & Wroth (1974) proposed that the value of tensile strain might be considered as the key indicator of structural damage, thus opening the way for much simpler assessment of the structural behaviour.

Following this idea, and considering the indications by Boscarding & Cording (1989) on the values of limiting horizontal tensile strain, Burland (1995) extended the previous classification of damage, to provide so-called "interaction diagrams" in which the identification of the category of damage results from the combination of the computed horizontal tensile strain and deflection ratio, see Figure 4.1. In this manner, assuming that a masonry wall behaves like a simple beam with bending and shear stiffness (Timoshenko beam), the category of expected damage can be evaluated in a relatively simple manner. This approach has been used extensively in the design phase of the Jubilee Line Extension in London, as an intermediate step of a process of damage assessment that included a preliminary estimate, based on the green field deformations, followed by more advanced analyses in which soil-structure interaction was taken into account.

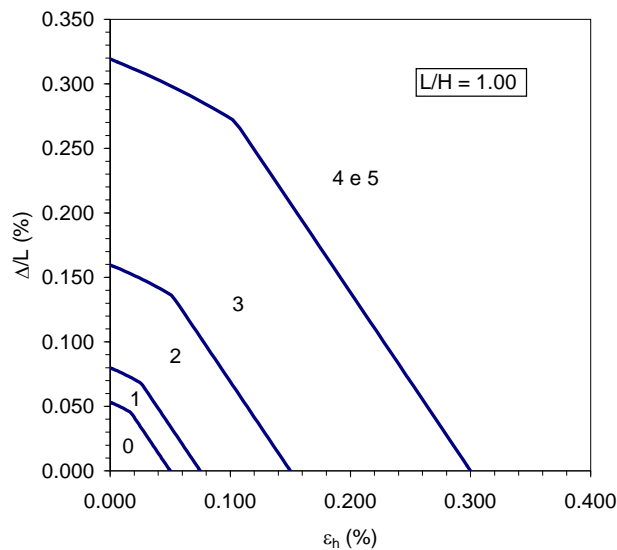


Fig. 4.1 – Interaction diagram and iso-damage zones for  $L/H = 1.0$ , after Burland (1995)

The extent to which the approach outlined above can be applied to the buildings of the centre of Roma and, more generally, the definition of a strategy for the preservation of their historical, artistic and monumental value are difficult issues that require appropriate consideration.

First of all, the construction of an infrastructure such as Line C of Roma underground, with a significant social impact, can only derive from the result of a careful cost/benefit analysis demonstrating that the benefits prevail. Therefore, society as a whole is called to carry the burden of the problems that may result from its construction and operation, provided, of course, that they are predicted in design and contained within acceptable limits.

The definition of "acceptable limits", however, may constitute a problem. When the potentially affected buildings are of outstanding value, an extreme position may be that of considering unacceptable any new work interacting with them, unless specifically intended for their preservation or valorisation. A striking example of this attitude is provided by the archaeological excavation required to expose the Arco dei Ladroni near Basilica di Massenzio, which re-

quired the installation of a loud and aesthetically questionable structural safeguard measure to minimise the risk of collapse of part of the monument.

If, on the one hand, the protection of the monumental heritage requires that the absence of damage due to the works be guaranteed, on the other hand this cannot mean the absence of any interaction between the new works and the old buildings. In the case at hand, more stringent constraints had to be introduced to ensure the best protection of the monumental heritage and a consistent and scientifically sound methodological approach developed to evaluate how the construction of the line would affect the existing historical buildings.

To this end, the analysis of the interaction between construction activities and built environment was carried out following procedures of increasing complexity, level of detail and accuracy.

#### 4.2 Methodological approach

The evaluation of the expected damage was carried out with reference to the classification of damage by Burland (1995) using analyses of different levels.

At a first level, simplified analyses were performed computing surface and near-surface displacements using the semi-empirical methods described above and neglecting the stiffness and the weight of the buildings (Attewell & Woodman, 1982, Attewell *et al.* 1986).

The resulting displacement field was applied by the structural engineering group to a 3D linear elastic finite element model of the structure under examination. Both the geotechnical and structural engineering groups carried out independent evaluations of potential damage to the buildings. To account for the historical value of the buildings, the values of limiting tensile strains adopted by the geotechnical engineering group to identify the damage categories were lower than those proposed originally by Boscardin & Cording (1989). Based on the outcome of the geotechnical and structural evaluations, the study ended if the damage was deemed negligible, or continued to a higher level of complexity (Level 2).

At this second stage, the interaction between the tunnels and the historical buildings was studied through 2D or 3D finite element analyses that considered soil-structure interaction adopting a simplified description of the mechanical behaviour of the buildings. The computed displacement field, accounting this time for the stiffness and weight of the building, was applied again to the structural model and damage was re-evaluated, independently, by both groups. Depending on the computed results, either damage was deemed acceptable, or prospective remedial techniques were indicated.

## 5 SOIL STRUCTURE INTERACTION ANALYSIS

Soil structure interaction studies require the definition of a computational strategy yielding the same level of approximation for both geotechnical and structural analyses. This requirement stems from two sets of problems. The first is connected with the specialization of the available numerical codes, which often makes it impossible, or at least very difficult, the task of tackling structural problems with "geotechnical" codes and vice versa. A second problem derives from the skills and sensitivity required to use effectively specialised software for the structural and geotechnical aspects. This suggested to carry out independent geotechnical and structural analyses, but also to define a procedure that would permit to study the interaction between the buildings and the ground with the same level of approximation for the geotechnical and structural aspects.

The soil-structure interaction analyses adopted a simplified mechanical description of the buildings, obtained representing the structure as an equivalent solid with simpler geometry and appropriate physical and mechanical properties. This equivalent solid has the same shape in plan as the real building it is meant to represent, is fully embedded into the soil and is assumed to behave as a linear elastic material. The equivalent solids are introduced in the geotechnical finite element analyses with equivalent stiffness and weight that reproduce those of the complete buildings. In this manner, the geotechnical analyses produce a displacement field that accounts for the stiffness and weight of the building and that can be eventually applied to the complete structural model for a final evaluation of the effects induced by tunnel construction.



Strictly, the assumption of linear elasticity for the equivalent solid is valid only when the structure undergoes small distortions. When the mechanical non-linearity of the real structure plays a major effect, in principle the procedure may require one or more iterations. However, the results of the analyses have proved that generally this is not the case, at least for relatively small volume loss.

### 5.1 Geotechnical models

To limit the computational effort, particularly for three-dimensional analyses, in a first stage of the study the soil was modelled as linearly elastic-perfectly plastic, with a Mohr Coulomb yield criterion. Subsequently, to overcome the limits of this constitutive law, the mechanical behaviour of all soils was described using an elastic-plastic rate independent constitutive model with isotropic hardening that is capable of reproducing the main features of the mechanical behaviour of soils, namely the *Hardening Soil* model (Schanz *et al.*, 1999), available in the library of the finite element codes Plaxis and Tochnog that were used for the numerical analyses.

In the constitutive model, the elastic behaviour is defined by isotropic elasticity using a stress dependent Young's modulus, while plasticity is governed by a deviatoric and a volumetric yield surface with independent isotropic hardening laws, related to deviatoric and volumetric plastic strains, respectively. The flow rule is associated for states lying on the volumetric surface, while a non-associated flow rule is used for states on the deviatoric surface.

Compared to linear elastic-perfectly plastic models, the use of *Hardening Soil* results in a significant improvement of the analyses because it considers a non-linear (hyperbolic) stress-strain relationship; takes into account the stiffness variation on plastic loading and unloading; considers the dependence of the stiffness on the current stress state and on the overconsolidation ratio; predicts the occurrence of plastic strains from the onset of deviatoric loading, even for overconsolidated states, thanks to the separation of the volumetric and deviatoric yield surfaces.

### 5.2 Structural models

In principle, the dual objective of modelling accurately the mechanical behaviour of masonry and of identifying potential damage, even at the level of the structural detail, would imply the use of three-dimensional non-linear numerical analyses. As the buildings potentially affected by construction of Contracts T2 and T3 and deemed worthy of attention are numerous, it was not possible to carry out this type of analysis for all of them and this approach was followed only in some specifically selected cases.

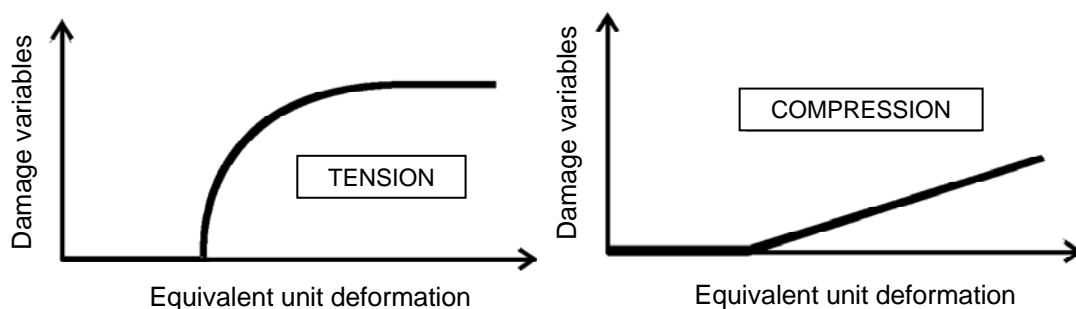


Fig. 5.1 - Damage variables, after Mazars (1984)

A reasonable balance between the computational restrictions and the need to achieve the objectives of the interaction studies, was offered by an application of damage mechanics, that treats masonry as a continuum and introduces damage as a tensorial variable. In a simplified isotropic model proposed by Mazars (1984) for concrete, damage was represented by two independent scalar variables, describing the behaviour in extension and in compression, see Figure 5.1. This was the reference model adopted at the early stage of the study, within a research contract between the Municipality of Roma and the University (STA-DISG, 2003), considering

only damage in extension as the most relevant for masonry walls. In successive studies, the same model was also used to evaluate damage from the results of linear analyses.

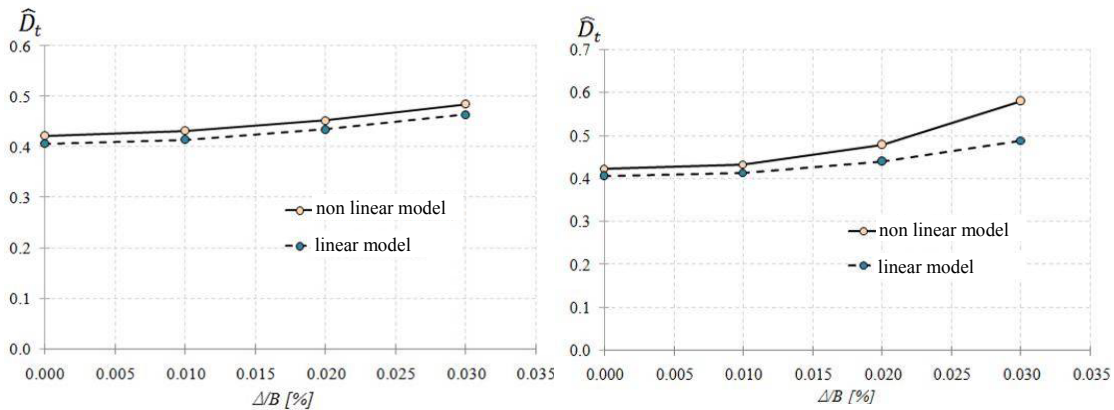


Fig. 5.2 – Parametric study of damage in masonry wall

The results of a parametric study of the behaviour of masonry walls with rectangular openings and different ratios of the void to masonry areas, shown in Figure 5.2, demonstrated that linear and non-linear models provide very similar results in sagging, while in hogging the results are in reasonable agreement only up to values of deflection ratio,  $\Delta/B$ , of  $1 \times 10^{-4}$ .

The results of this study suggested that it was possible to use linear models in all those cases in which Level 1 analyses indicated negligible damage, limiting the use of non-linear models to only a few cases, with the main function of support of the results of the linear analyses.

### 5.3 Equivalent Solids

The technical literature contains several examples of equivalent solids, typically used to model masonry structures in numerical geotechnical analyses. After the work by Burland & Wroth (1974), who used the simple Timoshenko beam to obtain their classification of damage, other Authors (Finno *et al.*, 2005; Pickhaver, 2006) have regarded the façades of masonry buildings as equivalent beams of appropriate shear and bending stiffness.

In the literature, it is generally recognised that the simple assumption of linear elastic isotropic behaviour does not describe the behaviour of real structures adequately, and that it may be necessary to adopt values of the ratio of the Young's and shear modulus,  $E/G$ , outside the permitted range of isotropic elasticity, depending on the type of building. For a linear elastic isotropic material with a Poisson's ratio  $\nu = 0.3$ ,  $E/G$  is equal to 2.6; however, for reinforced concrete frame structures, with a relatively high shear deformability, it is advisable to adopt values of  $E/G$  as high as 12.5, while for masonry structures the recommended values of  $E/G$  may be as low as 0.5.

Voss (2003) extended the work of Burland & Wroth (1974) to propose an expression for the deflection ratio,  $\Delta/L$ , in which the ratio  $E/G$  appears explicitly, together with the distance of the neutral axis from the bottom of the beam, normalised by the beam's height, see Figure 5.3.

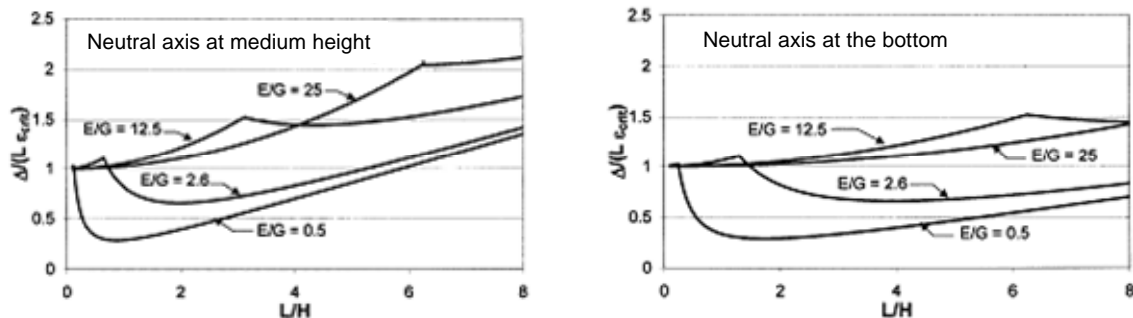


Fig. 5.3 – Deflection ratio as a function of  $E/G$  for an elastic beam, adapted from Voss (2003)

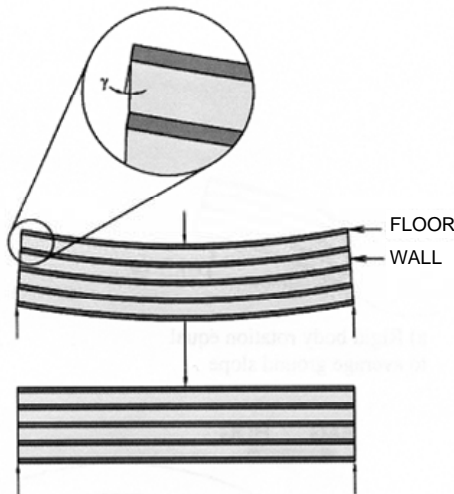


Fig. 5.4 – Scheme of laminated beam (Finno, 2005)

In the approach by Finno *et al.* (2005), the equivalent beam is identified assuming that the floors contribute to the bending stiffness of the building, while the walls contribute to its shear stiffness. The authors end up with a laminated beam model, see Figure 5.4, in which the different layers correspond to floors and walls.

In the work by Pickhaver (2006) the façades of the building are modelled as elastic beams, whose behaviour depends on the percentage of openings and on the mode of deformation.

Based on the results of an extensive parametric study of the behaviour of rectangular masonry façades with different percentage of openings, carried out with linear finite element analyses, Pickhaver (2006) demonstrated that: (i) the Timoshenko beam does not provide an adequate representation of the behaviour of the walls and (ii) there is a critical value of the ratio  $L/H$ , between the length and the height of the façade, below which the stiffness depends essentially on the ratio  $L/H$  and above which the stiffness depends essentially on the percentage of openings, see Figure 5.5. The Author proposed also a procedure to assess the equivalent values of the area and inertia of the cross section of the beam, to take into account the above-mentioned factors.

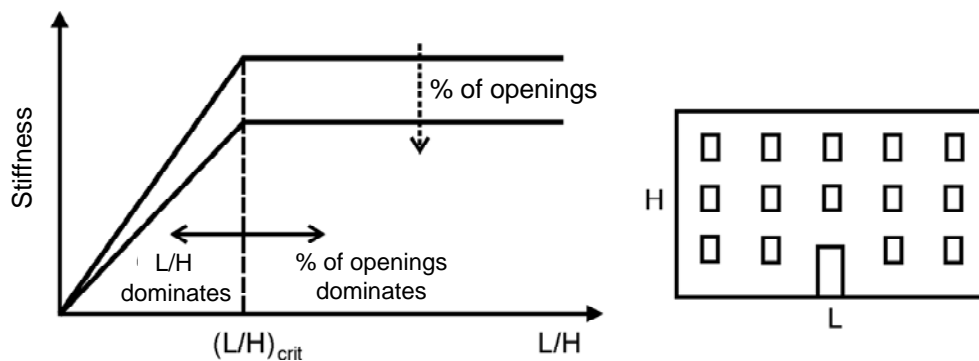


Fig. 5.5 – Effect of  $L/H$  and of percentage of openings on the stiffness of masonry walls, after Pickhaver, 2006)

In this study, the issue of the identification of the equivalent solid was addressed anew. In particular, it was assumed that the actual and the simplified structure can be considered equivalent if they show the same response to a given perturbation. For the present problem, the perturbation consists of imposing the vertical displacements computed in the green-field analyses at foundation level, and the corresponding response is the distribution of the nodal forces at the same level. The Young's modulus of the equivalent soil is found iteratively to produce a distribution of nodal forces at foundation level that matches the distribution computed using a complete structural model of the building, see Figure 5.6.



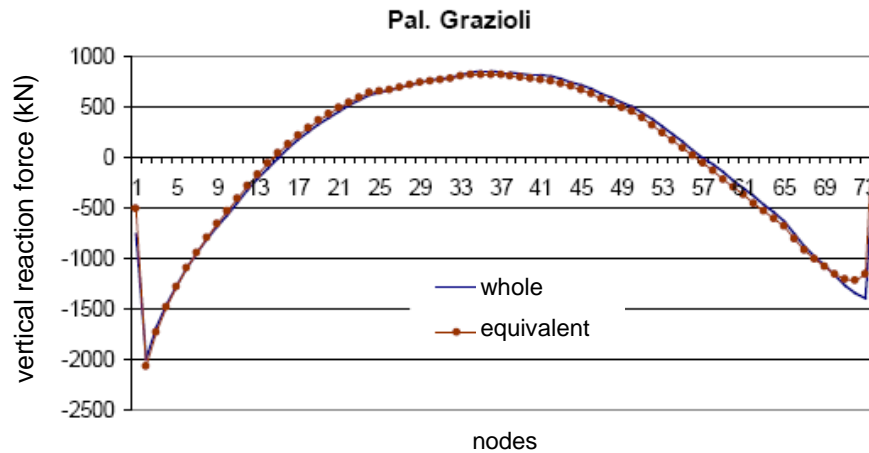


Fig. 5.6 – Example of calibration of the equivalent solid based on node reactions

The thickness of the equivalent solid has been generally chosen so as to occupy, in the mesh used for geotechnical soil-structure interaction analyses, the same space of the foundations of the real building.

## 6 BACKGROUND NOISE

In the context of this study, the term “background noise” signifies the variation in time, before construction, of all those physical quantities, such as surface movements and pore water pressures, which will be modified by the construction of the line. In the case under examination, it is very important to examine the background noise in terms of building settlements, as the background displacements can be of the same order of magnitude as those induced by construction.

A number of factors, such as the geological environment in which the city developed, the geotechnical characteristics of the foundation soils, the presence of the Tiber and the periodic fluctuations of its water level, and the daily and seasonal thermal cycles, combine to generate movements of the buildings.

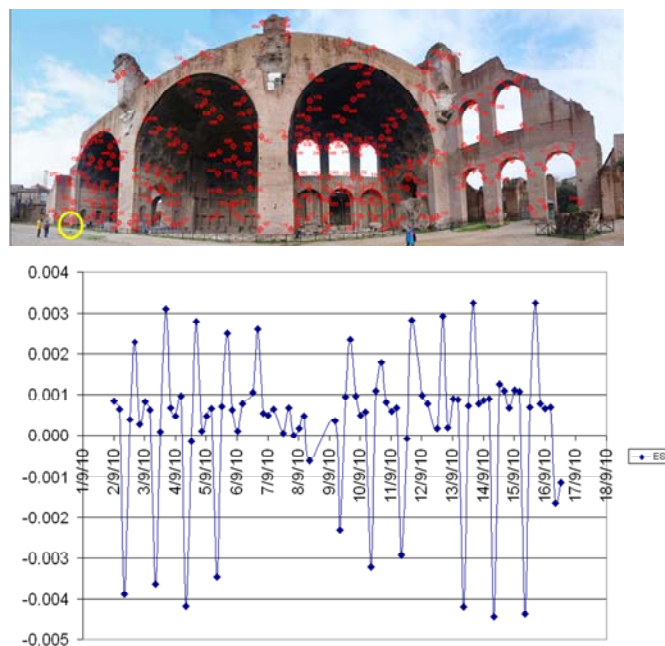


Fig. 6.1 – Effect of the daily thermal cycle on the displacements of Basilica di Massenzio

For instance, automatic total station monitoring of the Basilica di Massenzio revealed that the building experiences every day displacements of the order of millimetres, due to the daily thermal cycle (Figure 6.1).

The progressive settlements of Palazzo di Giustizia, before the reinforcement of its foundations, could be attributed to fluctuations in the hydrometric regime of the Tiber River (Calabresi *et al.*, 1980), see Figure 6.2. In fact, the same cause is responsible for the movements of a large number of buildings of different type and size, located along the river. As shown in Figure 6.2, the fluctuations in the hydraulic head in the layer of gravel and sand immediately above the base Pliocene clays follows the hydrometric level fluctuations in the Tiber River; this creates deformations of the overlying compressible soils and is responsible for the extension of the area of influence of the Tiber hydrometric level.

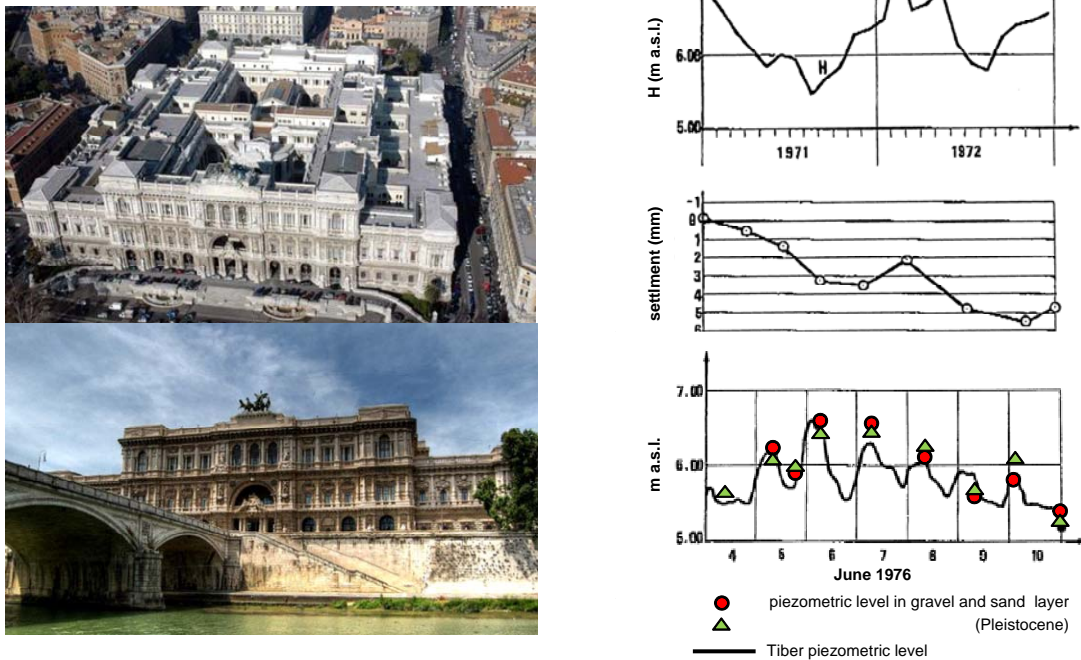


Fig. 6.2 – Vertical displacements of Palazzo di Giustizia due to fluctuations of the Tevere hydrometric level (after Calabresi *et al.* 1980).

Using a monitoring technique based on the creation of maps of surface deformation from SAR (Synthetic Aperture Radar) images, it is possible to obtain a very accurate representation of the elevation of numerous *permanent scatterers*, *i.e.*, details that always reflect the radar signal in the same way during different passages of the radar, such as rooftops or terraces of buildings. The technique can potentially measure millimetre-scale changes in deformation over spans of days to years.

Figure 6.3 shows an overall view of the permanent scatterers in the city of Roma; these are represented as small circles ranging in colour from blue to red depending on the measured value of the average annual rate of settlement. Consistently with what just discussed, it is possible to identify a strip along the Tiber characterised by higher than average values of annual settlement rate and some critical areas, typically corresponding to problematic foundation soils, where the buildings show significant ongoing settlements.

Taking a closer look to the buildings of historical centre, potentially affected by the construction of Contracts T2 and T3, the data in Figure 6.4 indicate that the foundation soils in the baroque bend of the Tiber are more compressible than the oldest soils between Piazza Venezia and Coliseum. Even at the scale of individual or adjoining buildings, SAR data show noticeable average settlement rates, up to 0.2 mm/year, and seasonal oscillations of the order of the millimetre, see Figure 6.5.

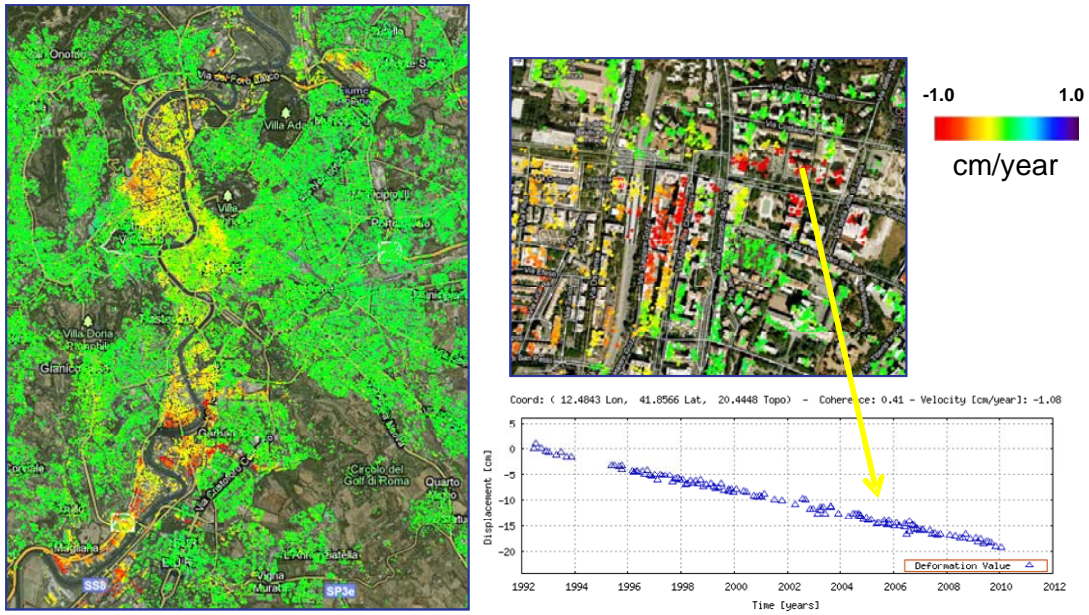


Fig. 6.3 – SAR survey: distribution of average annual settlement rates for the whole urban area.

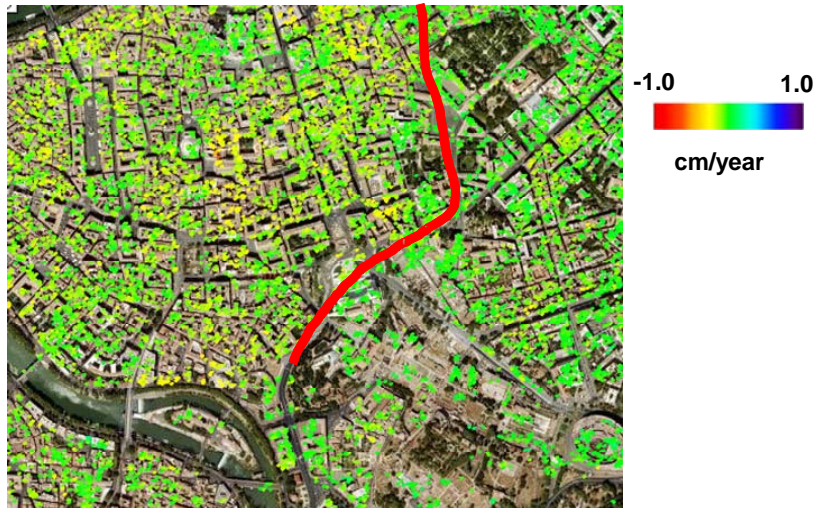


Fig. 6.4 – SAR survey: distribution of average annual settlement rates for Contracts T2 and T3

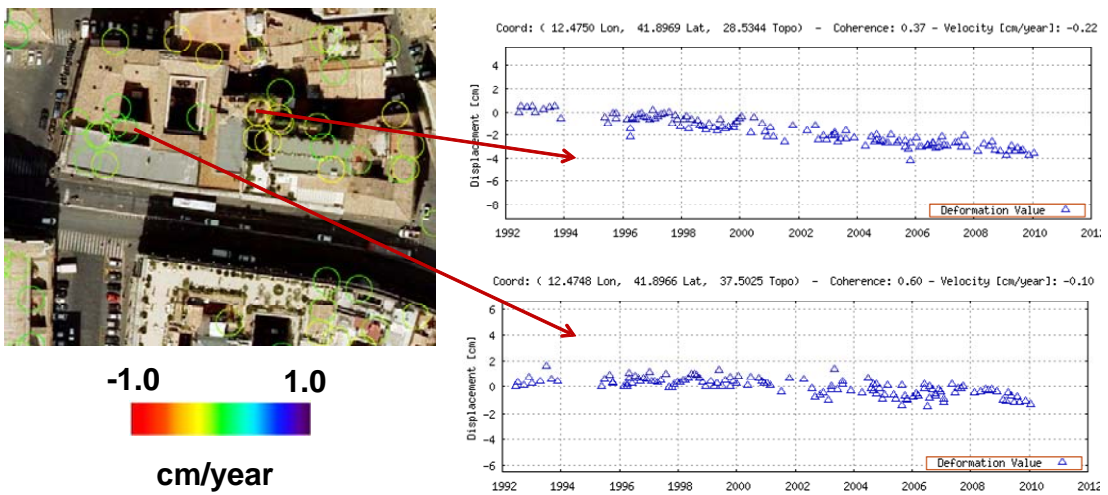


Fig. 6.5 – SAR survey: distribution of settlement rates at the single-building level



The magnitude of the measured background noise illustrated above suggests that it is probably pointless to try to predict the effects of the construction of the line with accuracies smaller than about one millimetre and to attach particular relevance to displacements of the order of a few millimetres in the assessment of potential damage.

## 7 EXAMPLES

### 7.1 *Basilica di Massenzio*

The Basilica di Massenzio is a very interesting example to illustrate the approach that was adopted in the study. In fact, this is a particularly heavy structure, with significant contact stress transferred to the soil by the foundations that consist of simple extensions of the bearing walls, with a very limited widening. Another reason of interest of this case study derives from the variety of solutions that were considered in the design of the tunnels and of the station shaft, that made it necessary to carry out several interaction analyses.

#### 7.1.1 *History*

Construction of the Basilica began on the northern side of the forum under emperor Massenzio in 308, and was completed in 312 by Costantino I, after his defeat of Massenzio at the battle of Ponte Milvio.

In its original configuration, the building consisted of a central nave, covered by three vaults on four large piers and ending in an apse at the western end, and two flanking aisles spanned by three semi-circular barrel vaults perpendicular to the nave. Excluding the apses, the building occupied a rectangular area of about 80×60 m<sup>2</sup> (Fig. 7.1).

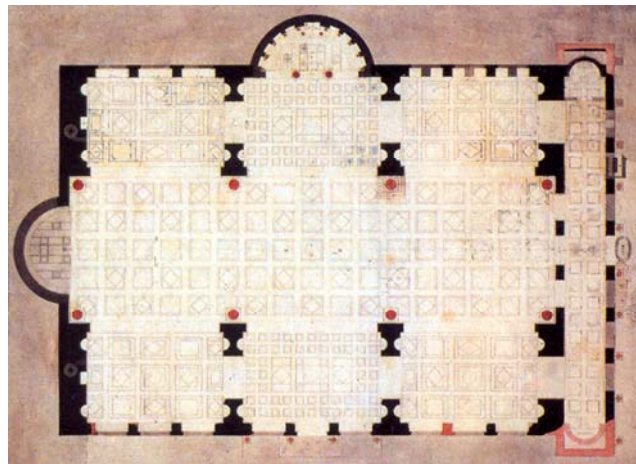


Fig. 7.1 – Map of Basilica di Massenzio after the restoration works of IV and V Centuries

Structural failures of the building occurred as early as during construction, probably during the interruption of the works for the civil war between Costantino I and Massenzio. Subsequent reinforcements included the construction of buttresses and contrast arches.

The perimeter walls of the Basilica, as well as the internal baffles, consist of two facings of clay bricks (*opus testaceum*) and a core of Roman conglomerate of lime and pozzolana (*opus caementicium*) including aggregates of different materials. The vaulted structures as well as the foundations are made in *opus caementicium*. The ceilings of the barrel vaults show advanced weight-saving structural skill with octagonal ceiling coffers.

In the fourth and fifth centuries the Basilica underwent several modifications, including the creation of the apse on its northwestern side, and the construction of a retaining wall to support the Velia Hill. In the sixth century, the Basilica had been already abandoned.

Subsequent repeated stripping and invasive crafts established on the site led to a progressive deterioration of the monument; the south and central sections were probably destroyed by the

earthquakes of 847 and 1349. In the following centuries, what was left of the monument was affected by progressive accretion and improper utilisation, including use as stable and riding school (Fig. 7.2).



Fig. 7.2 – View of the monument in 1865



Fig. 7.3 – View of the monument in 2000

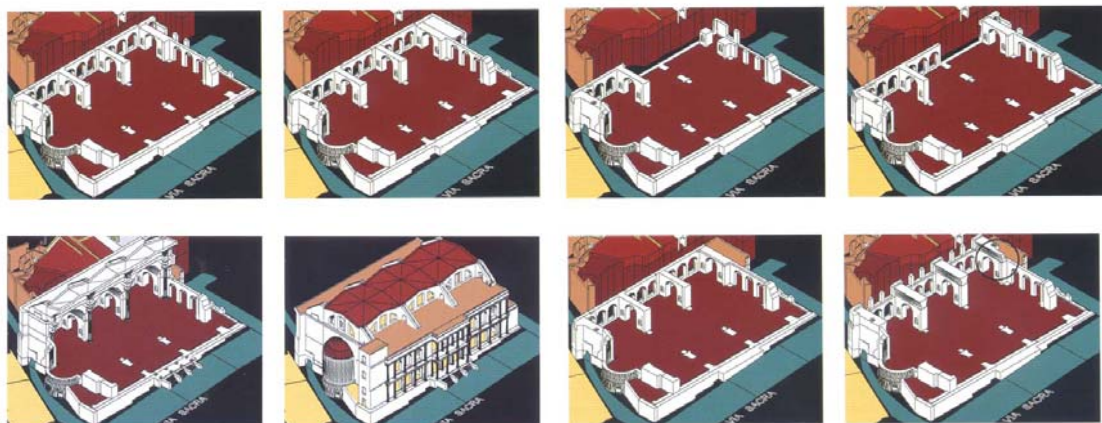


Fig. 7.4– Construction stages of Basilica di Massenzio



The first excavations to restore the Basilica to its original level began in the nineteenth century and in 1932 the excavation works to remove the Velia Hill and make room for the new Via dell'Impero were carried out; exposed by these works, the structure revealed the presence of an extensive pattern of cracks and significant damage in the two vaults and the apse.

In the 1960s, Musumeci reconstructed the destroyed dome of the apse in reinforced concrete; the present aspect of the Basilica is that reported in the photo of Figure 7.3.

Finally, Figure 7.4 illustrates the construction stages of the Basilica, which were used for its structural modelling.

### 7.1.2 Ground conditions

The geotechnical characterization of the foundation soils of the Basilica was undertaken using the results of site and laboratory tests carried out during several geotechnical investigation campaigns. Figure 7.5 shows a plan view of the Basilica and of the running tunnels together with the location of all the boreholes and *in situ* tests. The same figure also shows the position of three reference sections used for the interaction analyses, while Figure 7.6 details the stratigraphy along the central transversal section, intersecting the apse.

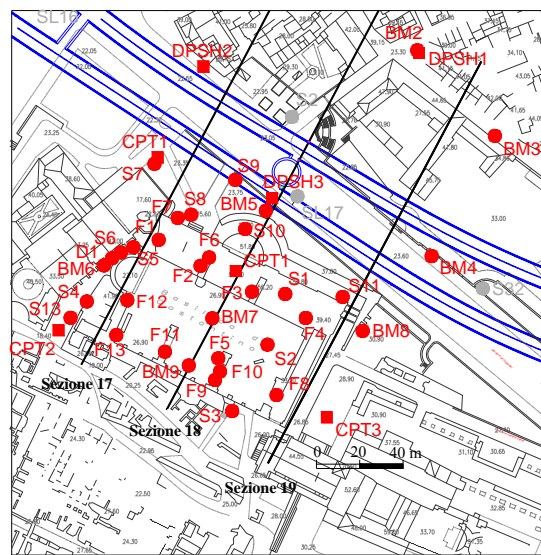


Fig. 7.5 – Geotechnical investigations in the area of Basilica di Massenzio

In the preliminary design, the tunnels had an external diameter of approximately 10 m, and run at a distance of 24 m from one another at a depth of about 25 m below the ground surface on Via dei Fori Imperiali. The distance of the axis of the closest running tunnel from the apse was about 22 m.

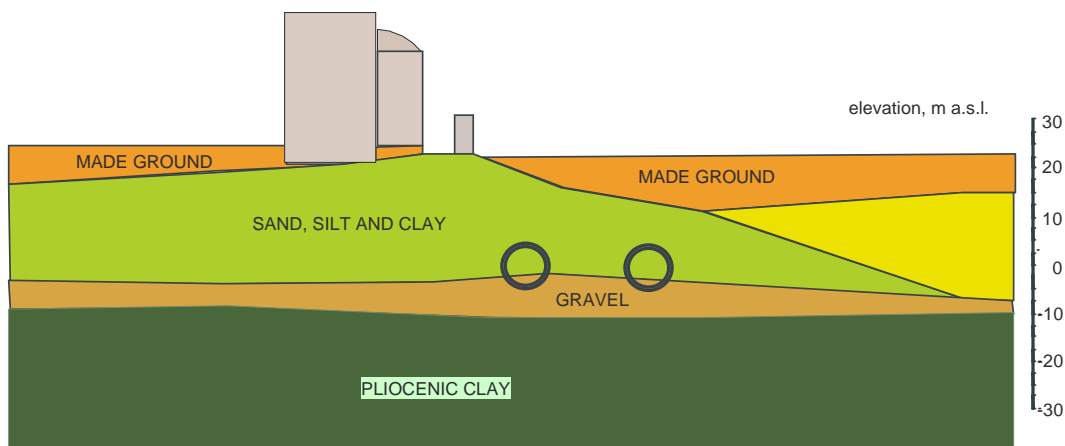


Fig. 7.6 – Stratigraphic profile along the central transversal section

Figure 7.6 shows the stratigraphy in the direction orthogonal to the tunnel axis, and the very variable thickness of the made ground and of the medium and fine grained soils of the Palotevere. The tunnels are mainly contained into these soils, with only their bottom part lying into the layer of gravel and sand at the bottom of the Paleotevere, immediately above the base formation of the Pliocene clay.

Figure 7.7 summarises the main index and physical properties of the foundation soils together with the groundwater pressure distribution, which is nearly hydrostatic with a level of about 15 m a.s.l.. The strength and compressibility characteristics are given in Figure 7.8. From the profiles in Figures 7.7 and 7.8 it is possible to recognise the Pleistocene and Pliocene formations and their different degree of overconsolidation.

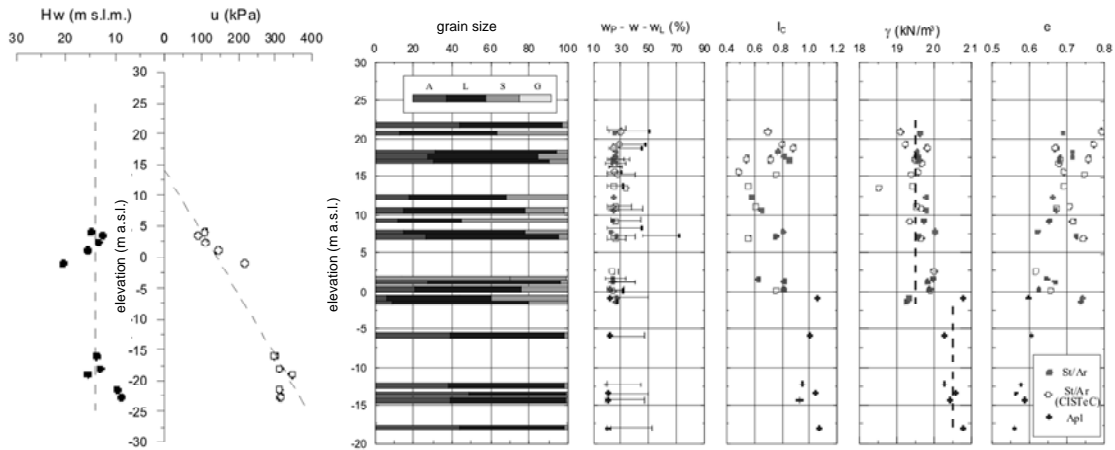


Fig. 7.7 – Geotechnical characterisation: groundwater pressure and main index and physical properties

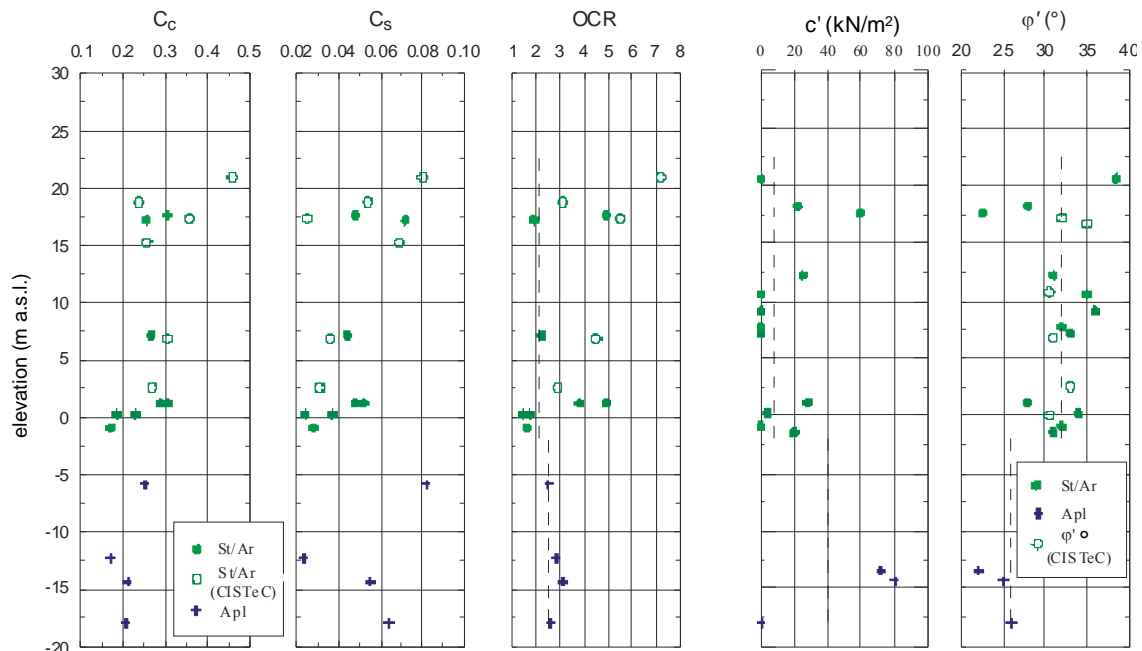


Fig. 7.8 – Geotechnical characterisation: strength and compressibility characteristics

### 7.1.3 Green field settlements

Figure 7.9 shows the contours of green-field settlements, in mm, computed using the empirical relationships described above. The contours refer to the end of construction of both running tunnels and are computed at the average foundation level using a volume loss  $V_L = 0.6\%$ . The



Following the methodological approach described above, the green field displacements were applied by the structural engineering group to both linear and non linear finite element models of the Basilica; Figure 7.11 and 7.12 show a selection of results of the structural analyses, in terms of contours of computed tensile strains in the structure.

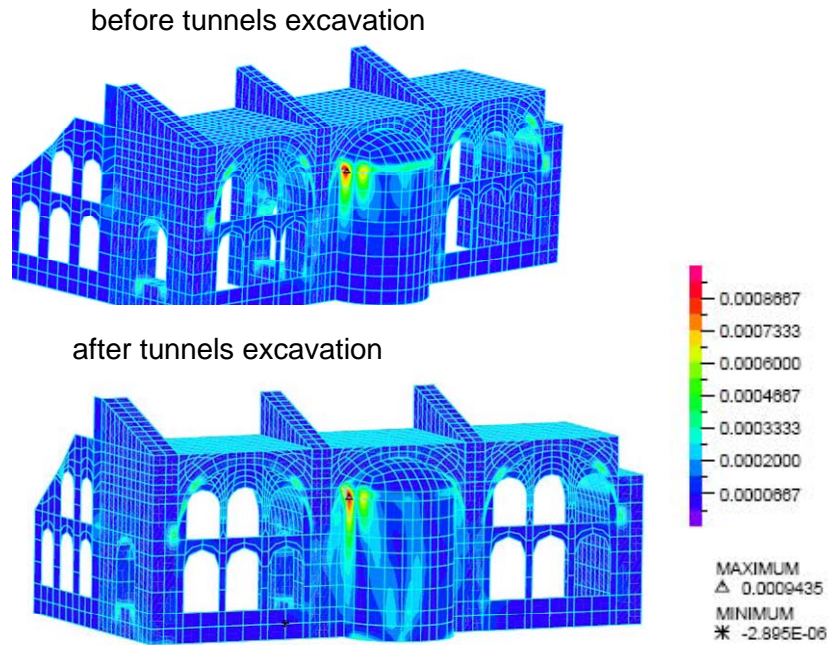


Fig. 7.11 – Level 1 structural analyses (linear model): contours of tensile strain

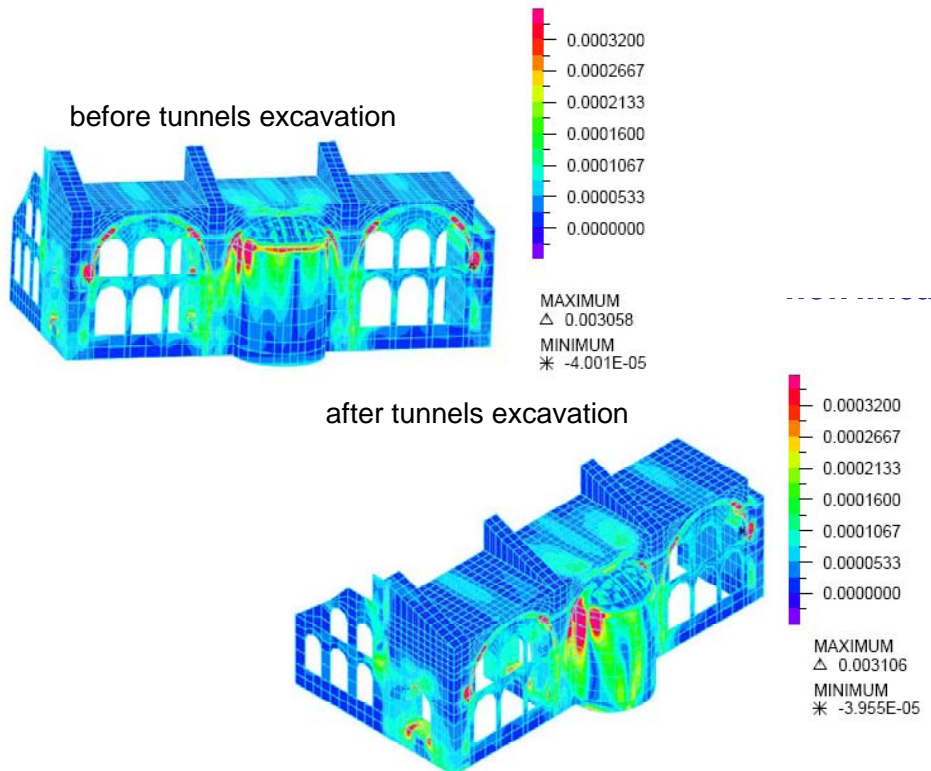


Fig. 7.12 – Level 1 structural analyses (non-linear model): contours of tensile strain

The results obtained using the linear model indicate that the most critical conditions occur for the apse, particularly at the junction with the recent reinforced concrete dome. It is worth noting that the state of stress in the structure is mainly due to self-weight and that it is only slightly modified by the displacements induced by tunnelling. In fact, the maximum tensile strain in the structure before the passage of the tunnels is equal to  $8 \times 10^{-4}$ , and increases to a value just larger than  $9 \times 10^{-4}$  (see Figure 7.11); before the construction of the tunnels, according to Burland's classification, the structure already is in a state of slight damage, and the category of damage is not worsened by the works.

The maximum tensile strains obtained from the non linear analyses are generally larger than those obtained using the linear model, but, once again, these are mainly due to self weight; the maximum tensile strains in the monument after construction of the tunnels increases from  $3.06 \times 10^{-3}$  to  $3.11 \times 10^{-3}$ , or a potential severe damage (Category 4). However, the incremental tunnelling induced damage can be considered negligible.

### 7.1.5 Level 2 analyses

Level 2 analyses were carried out using models of increasing geometric complexity. The behaviour of the soils was always modelled as elasto-plastic using the Hardening Soil model; the values of mechanical parameters were obtained from the available *in situ* and laboratory tests.

A first set of analyses was carried out in plane strain conditions, in the three sections indicated in Figure 7.5, orthogonal to the tunnel axes and through the piers of the Basilica. As the plane strain analyses assume that the structure is continuous in the longitudinal direction, it was necessary to scale the stiffness and weight to establish equivalence between the 3D signatures of the structure and its 2D representation.

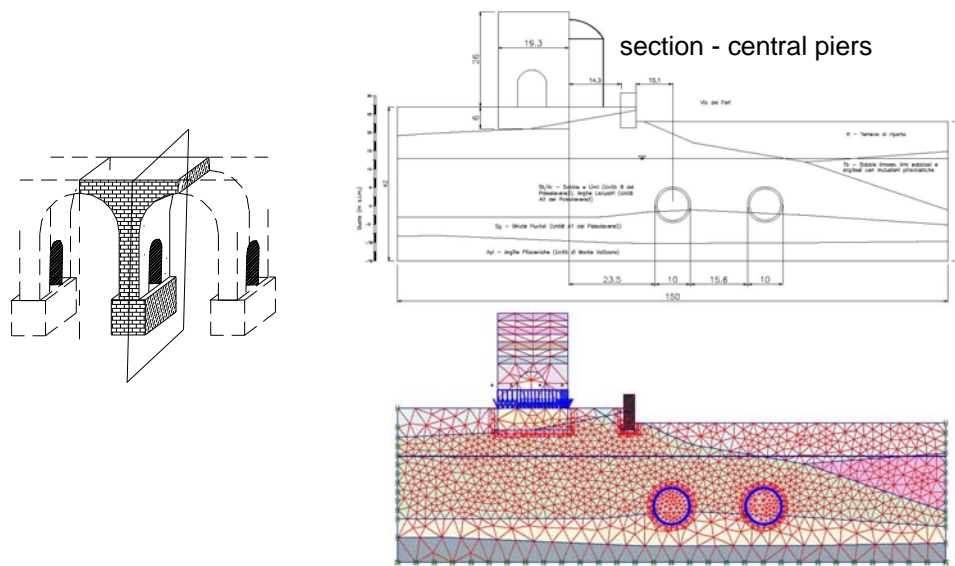


Fig. 7.13 – Level 2 geotechnical analyses, plane strain model

Figure 7.13 shows the cross section of the Basilica through the central pier, together with the mesh used in the numerical analyses; in the same figure, a diagram illustrates the geometric assumptions adopted in the factorisation of the weights.

A selection of the results of the plane strain analyses are given in Figure 7.14; these results confirmed that the strain level in the piers is rather small, as expected from Level 1 analyses, but also provided evidence of some unexpected behaviour.

As illustrated in Figure 7.14, the vertical displacements of the pier reach a value of about 6 mm and are significantly larger than the corresponding settlements in green field, contradicting the common belief that green field analyses are more conservative than interaction analyses. The reason for this unusual behaviour, unique in all the studies carried out for Contracts T2 and T3, must be sought for in the structural features of the Basilica. As a matter of fact, this building has an extremely small value of the ratio of the area of the bearing structural members to the total covered area (about 12%, compared to, e.g., 23% of the Pantheon and 26% of S. Peter's Ba-



silica); this is likely to be responsible for its high structural vulnerability and the many collapses experienced through the course of its history.

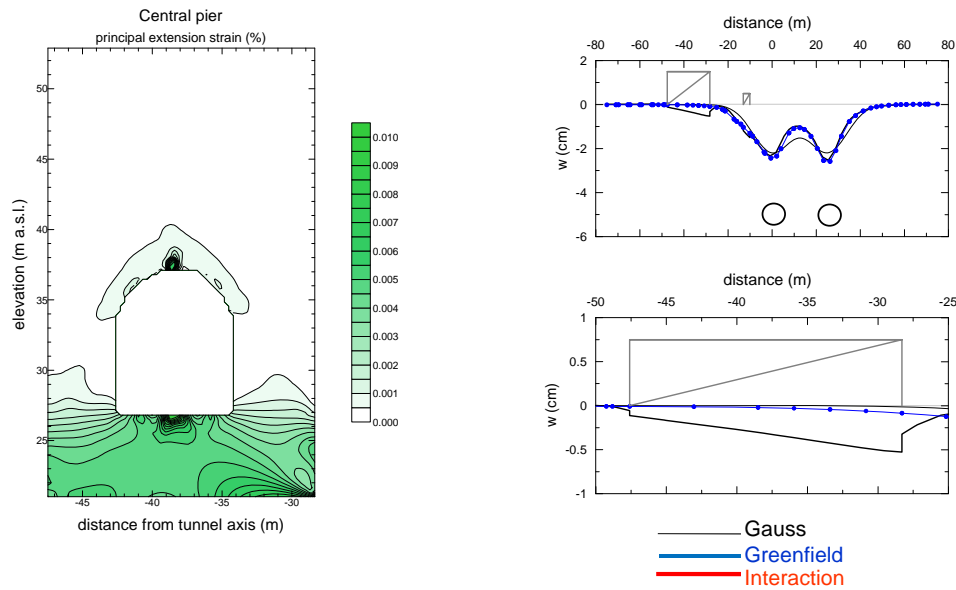


Fig. 7.14 – Results of plane strain Level 2 geotechnical analyses

Because of the significant weight of the structure, the foundation soils experience significant deformations, considerably reducing their shear stiffness. This reduced stiffness is well reproduced by the constitutive model used in the numerical analyses, which accounts for the dependency of soil stiffness on strain level, so that even the relatively small changes of stress state at foundation level due to the excavation of the tunnels produce appreciable settlements due to the reduced local values of the shear stiffness.

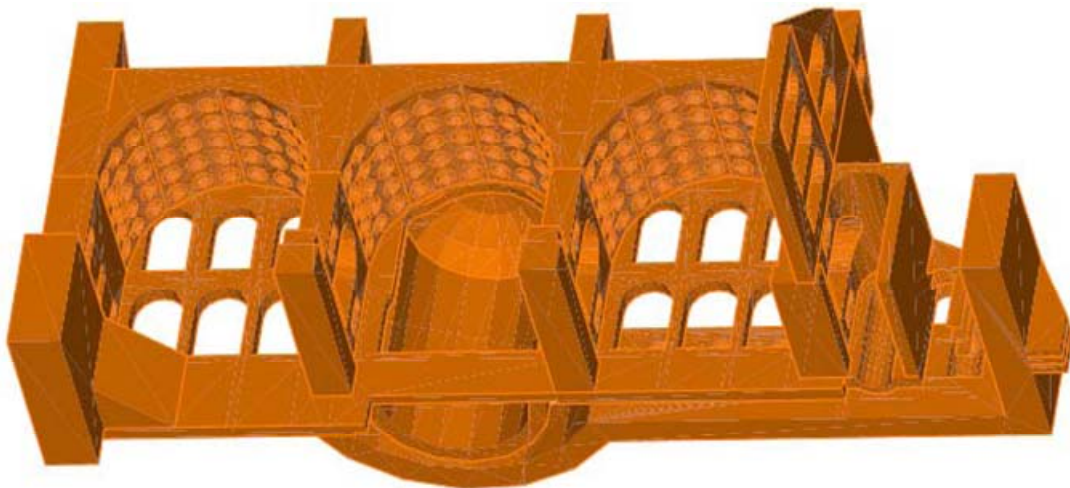


Fig. 7.15 – Reference geometrical model for Level 2 structural analyses

Level 2 structural analyses were carried out using a more detailed three-dimensional model of the monument (see Figure 7.15) while additional three-dimensional soil-structure interaction analyses were performed by the geotechnical engineering group in which the structure was replaced by an equivalent solid (see Figure 7.16).

The results of these analyses are shown in Figure 7.17, with reference to the same cross-section considered above and a longitudinal section corresponding to the façade of the Basilica. The results, comparable with those obtained with the 2D analyses, confirm the relatively large settlements of the foundations of the transverse piers, with the exception of the Carinae pier; this

is probably due to the fact that this pier is founded at a larger depth than the other two and induces smaller shear stress in the foundation soils that suffer to a lesser extent by shear stiffness degradation.

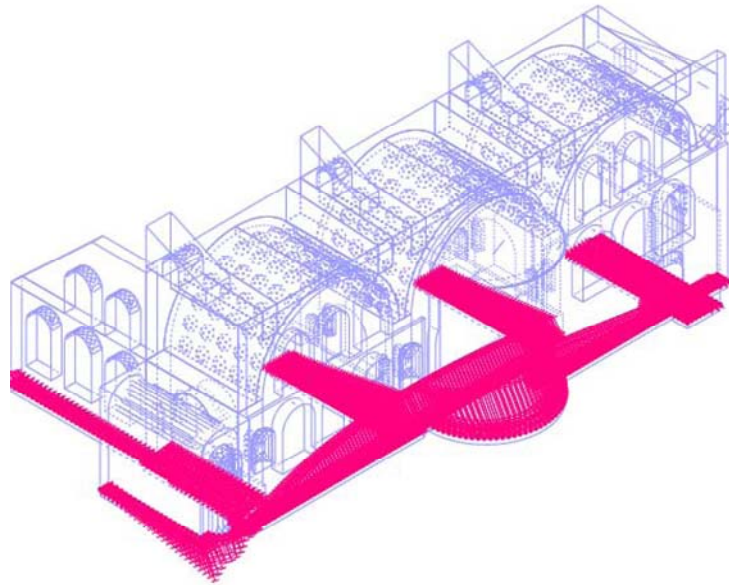


Fig. 7.16 – The equivalent solid for Basilica di Massenzio

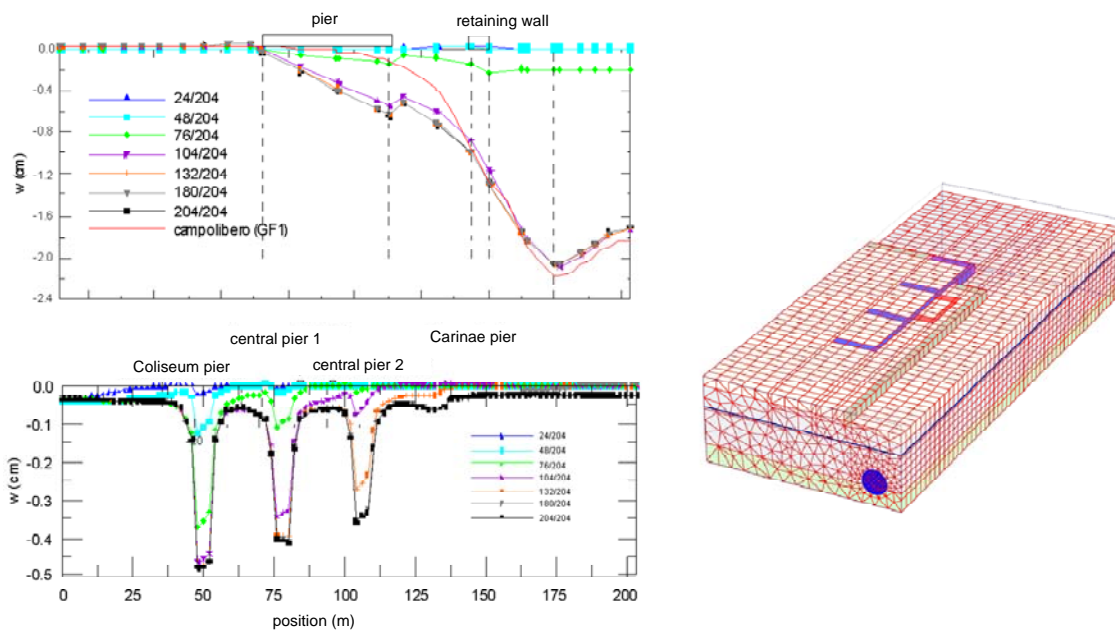


Fig. 7.17 – Level 2 interaction analyses: vertical displacements of the foundation of Basilica di Massenzio obtained using equivalent solid

Figure 7.18 shows the results of Level 2 structural analyses in terms of contours of tensile strain, this time using a more reliable structural model in which material properties were obtained from a number of mechanical tests of samples of the masonry and non-destructive site investigations.

The results of all the analyses described above confirm the high vulnerability of the building, that must be considered as a unique case from the point of view of its structural behaviour, and demonstrate the validity of the approach taken on structural damage and its modelling, that should use non-linear models in the presence of a non negligible expected damage.

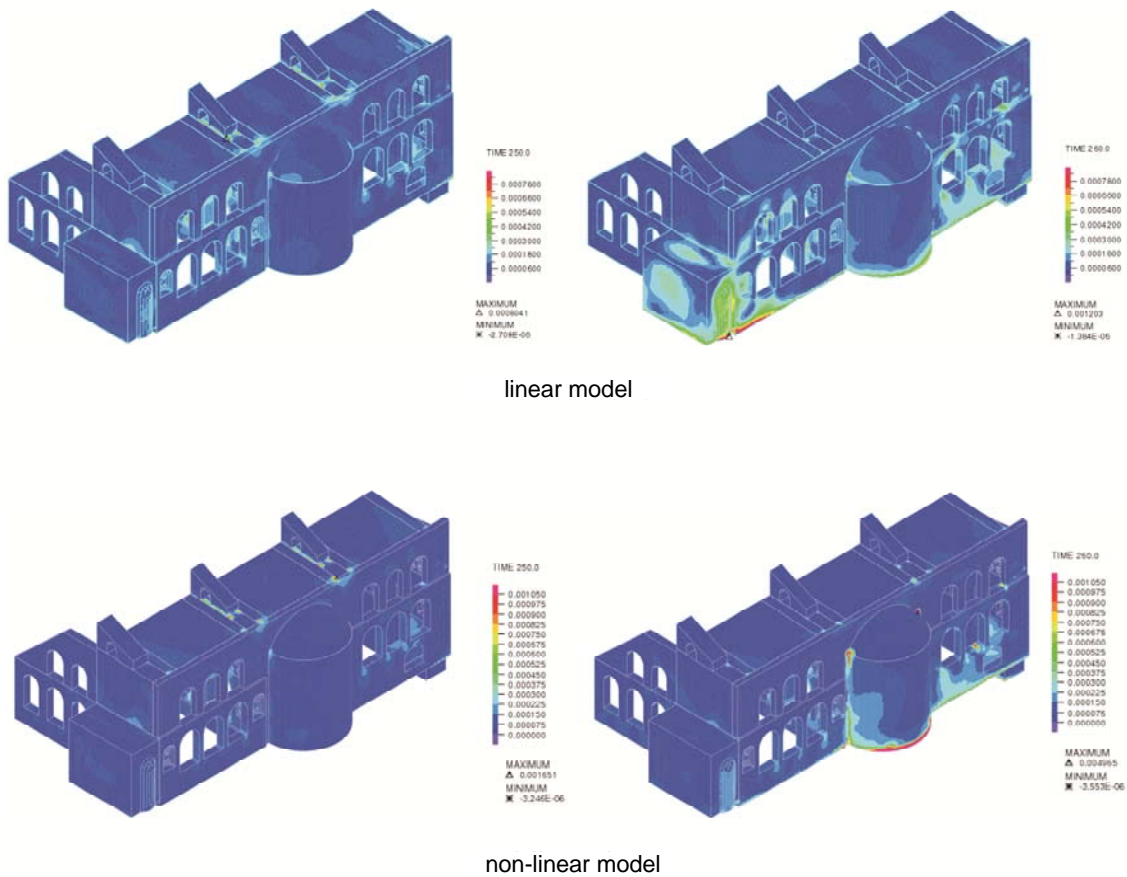


Fig. 7.18 – Level 2 structural analyses: tensile strains: (a) before and (b) after tunnel excavation

As a final comment it is worth to mention that successive modifications of design have led to a substantial reduction of the diameter of the running tunnels, with significant benefits on the potential damage to the monument, which is still receiving special attention and will require the implementation of protective measures.

## 7.2 Amministrazione Doria Pamphili

The second example that will be presented in some detail is that of the seat of the Amministrazione Doria Pamphili included in Contract T2 and located on Via del Plebiscito between Via della Gatta and Vicolo Doria, see Figure 7.19

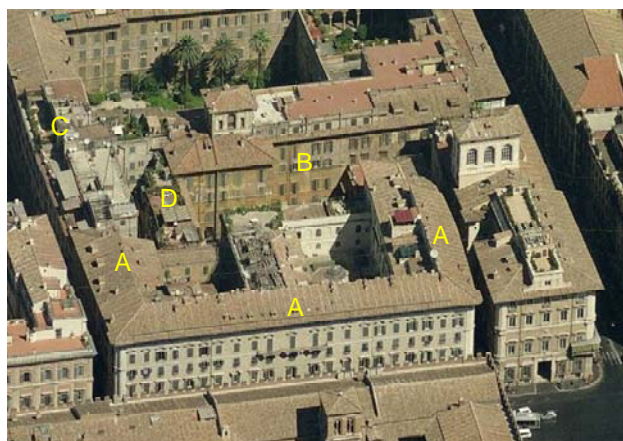


Fig. 7.19 – The building of the Amministrazione Doria Pamphili





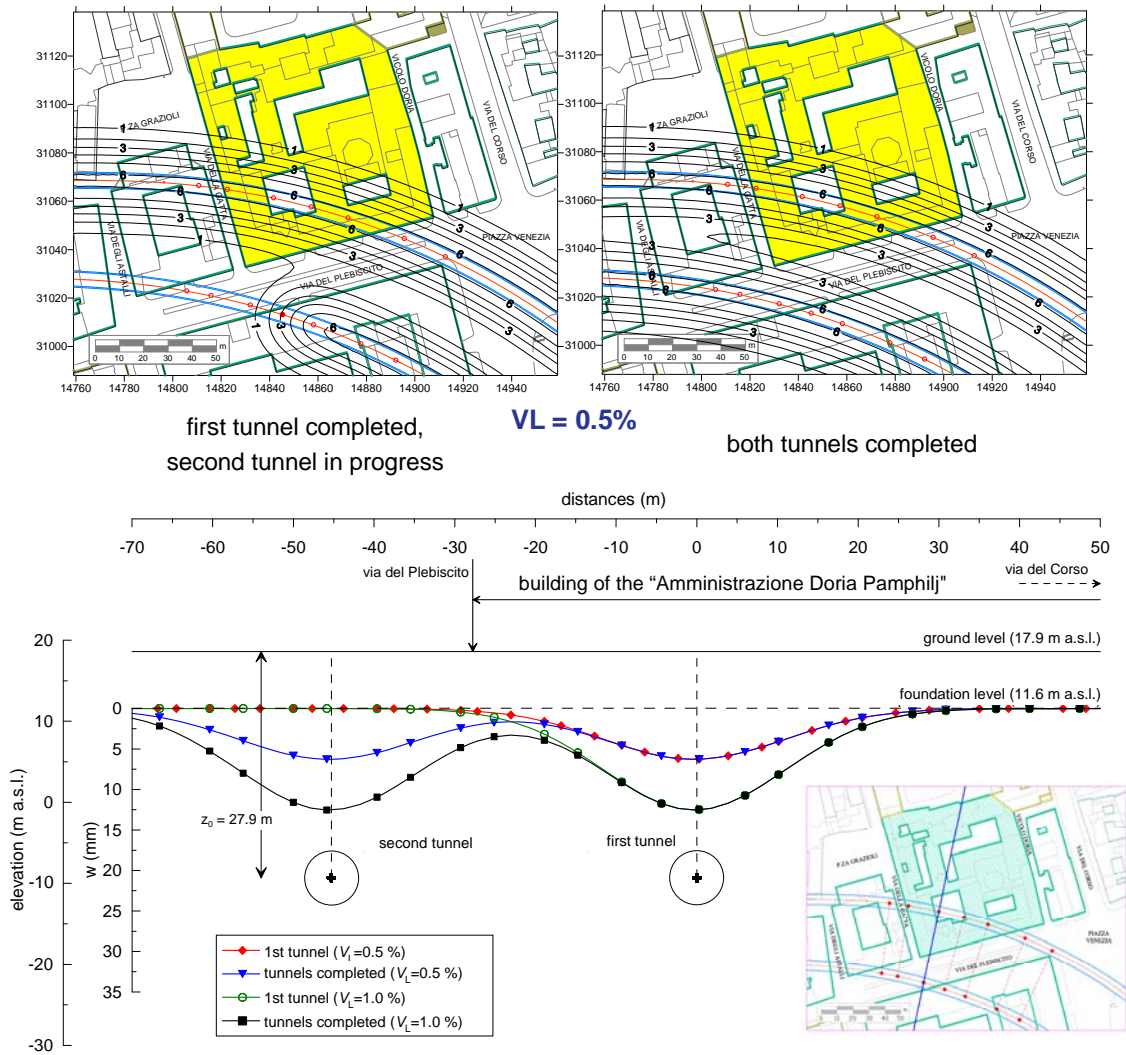


Fig. 7.21 – Subsidence trough and settlement profiles in greenfield conditions.

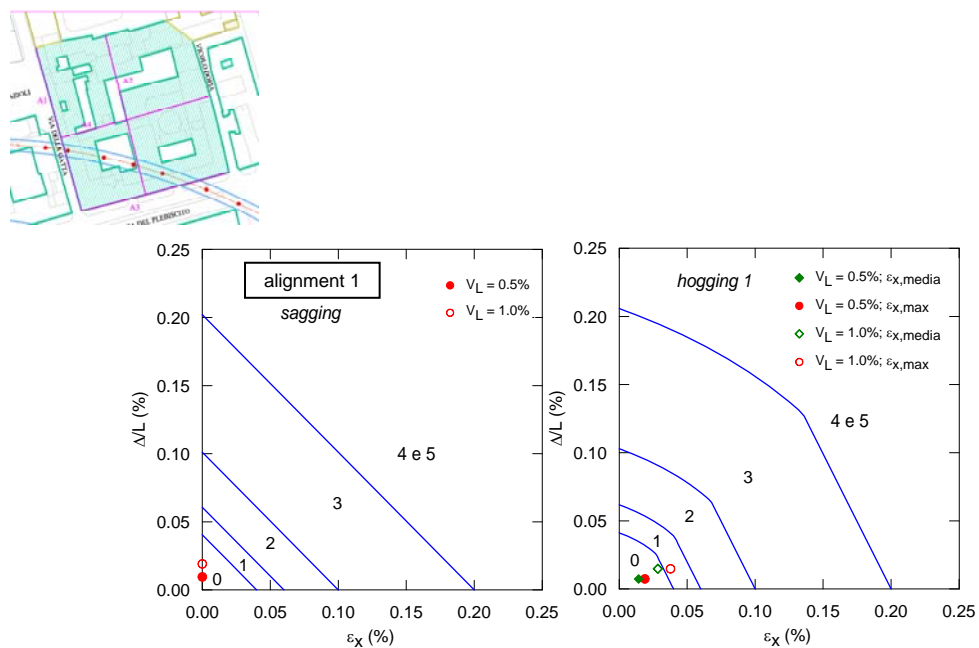


Fig. 7.22 – Expected damage corresponding to greenfield subsidence profile.



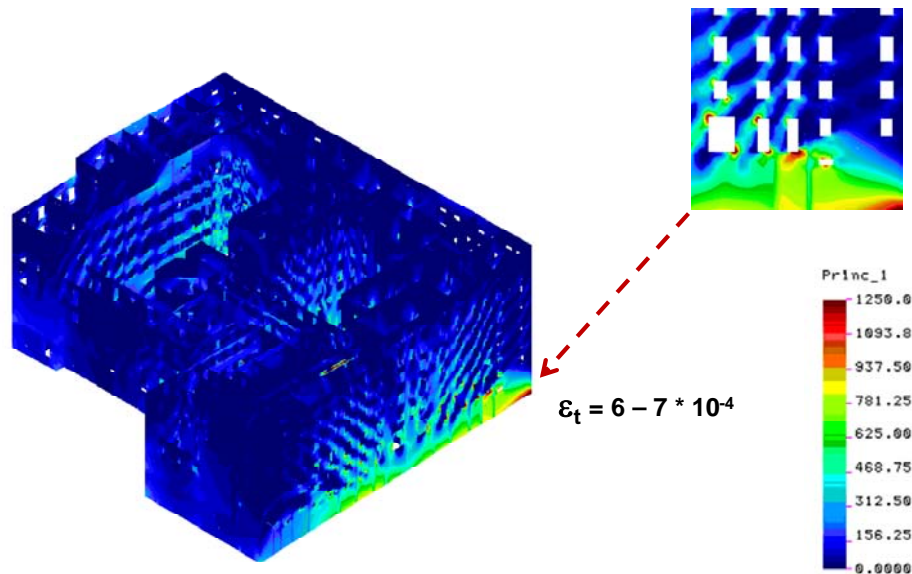


Fig. 7.23 – Level 1 structural analyses: maximum tensile stress for 1.0 % volume loss

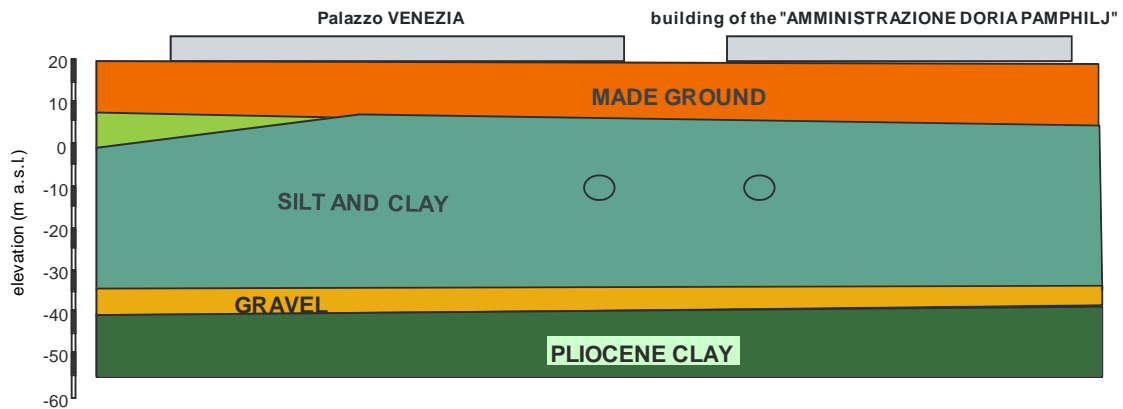


Fig. 7.24 – Stratigraphic profile along section 11 of Figure 7.19

Figure 7.27 shows the results of the three-dimensional interaction analyses in terms of computed settlements and tensile strains along the most critical section (section 1). The building deforms both in hogging and in sagging, with short term settlements of the order of 10 mm, and long term settlements almost twice the short term value, due to radial seepage towards the tunnel and consolidation.

Even with relatively high values of absolute and differential settlement, the tensile strains in the structure are rather small and, for a volume loss of 0.5%, the estimated damage is negligible. Also, although long-term effects produce a significant increase of the settlements, their effect on the estimated potential damage is beneficial, as they reduce differential settlements and curvatures.

Figure 7.28 shows a selection of the results of Level 2 structural analyses, confirming the conclusions obtained from the geotechnical analyses, regarding the magnitude and distribution of the tensile strain in the structural members; once again, it is found that the tensile strains are reduced in the long term.

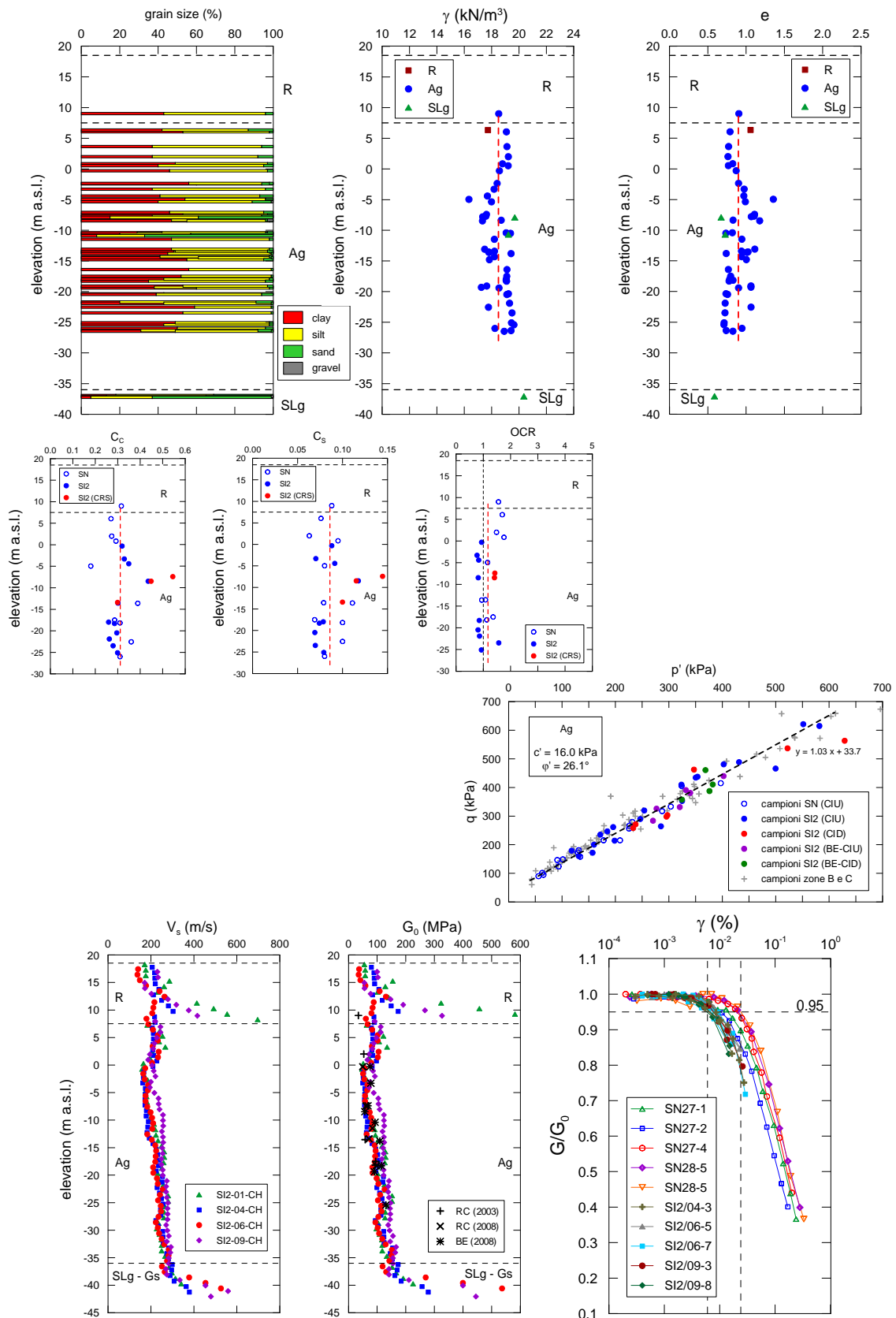


Fig. 7.25 – Geotechnical characterisation of the subsoil in the area of Piazza Venezia

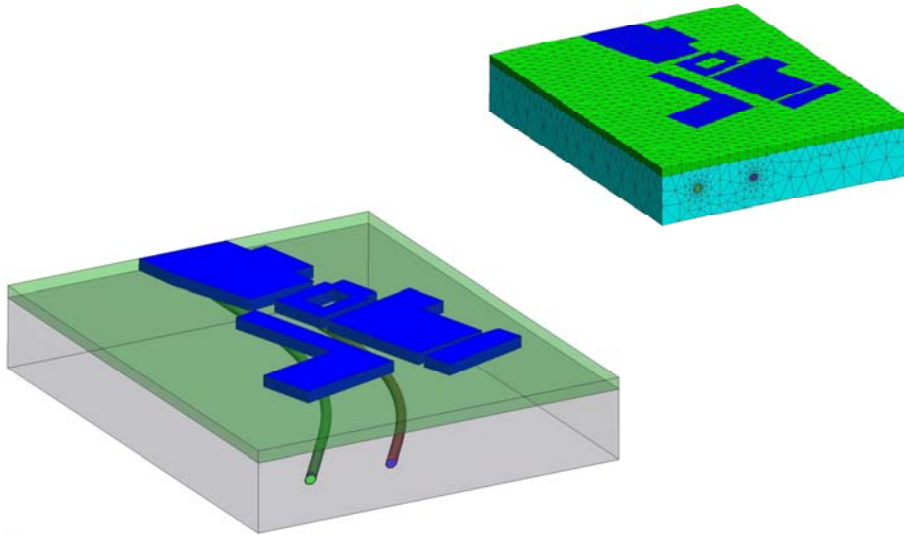


Fig. 7.26 – Three dimensional mesh and equivalent solids used for Level 2 geotechnical interaction analyses

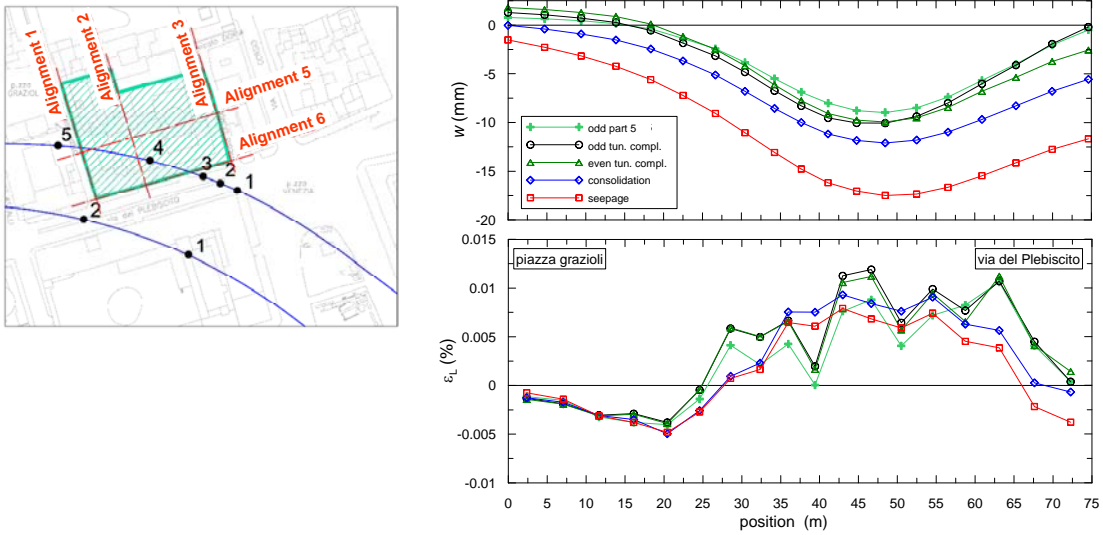


Fig. 7.27 – Results of 3D geotechnical analyses along the most critical direction (alignment 1).

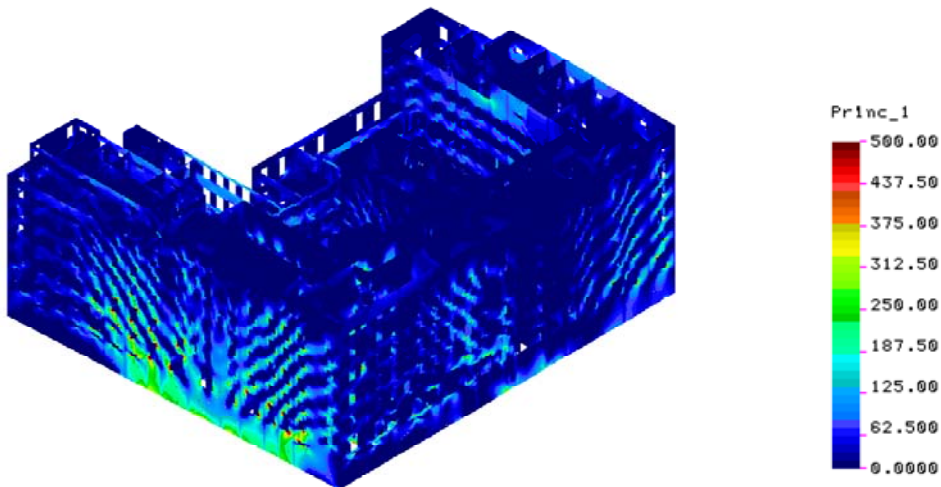


Fig. 7.28 – Results of Level 2 structural analyses

## 8 MONITORING AND MITIGATION MEASURES

In a work of such importance, monitoring plays a strategic role for different objectives, such as the quantification of the background noise prior to construction, the corroboration of the design predictions, the validation of the models developed for the interaction analyses and the calibration of geotechnical parameters, the support to decision-making for the implementation of mitigation and protective measures.

All of these activities require monitoring devices targeted for the specific objective and monitoring must be scheduled to take place with different frequencies in time.

In general, geotechnical and structural monitoring require the use of standard equipment for the measurement of rotations, surface and subsurface displacements, pore pressures, and the opening of structural joints and cracks. A common feature of all these monitoring systems is the required accuracy, because of the small effects expected from the construction of the line. The robustness and durability of the instrumentation are also of importance, in view of the long observation times; for example, pore pressure measurements will have to be extended after the end of construction to monitor long-term effects.

Another factor to consider is the advancement rate of the TBM, of the order of tens of meters per day, which imposes intense monitoring sessions during the passage of the tunnel face near the monument under examination and that renders it difficult to read those instruments, such as manual inclinometers and extensometers, that require relatively long measurement times. This is why the installed instrumentation should include automatic instruments such as electric piezometers and multi-base extensometers and inclinometers.

The extension and importance of the works and the need to protect the existing structures also suggest the installation of a geomatic net of automatic total stations, see Figure 8.1.



*Fig. 8.1* – Location of a motorized total station for the automatic measurement of the displacements of the surrounding buildings

These are a very effective means for the automatic measurement of the position in space of targets (retroreflector prisms) located in large numbers on the façades of the buildings at distances of up to a hundred meters. The most recent and advanced total stations reach an accuracy ranging from a few tenths of a millimetre to a few millimetres; the upper bound of this range can be reduced with specific statistical elaboration of the data to bring the variations of the coordinates within a predetermined level of probability. This requires high level data management skills and advanced geomatics knowledge, and a specific Working Group, devoted to Geomatics, had to be set up.

As already mentioned, one of the main objectives of monitoring is to provide support to decision-making for the implementation of mitigation and protective measures. This is the classical

use of monitoring under the observational approach in geotechnical design, which will be applied for the implementation of any measure intended to safeguard the monuments.

An example of mitigation measure typically carried out using the observational approach is that of compensation grouting. Before describing this technique, it may be useful to return to the criteria for the assessment of potential damage.

The current criteria for the classification of damage are based on the ease of repair. Excluding very severe damage, which clearly has irreversible consequences, the adoption of these criteria implicitly accepts that a building can always be repaired, classifying the severity of damage on the basis of the costs of the required interventions.

This pragmatic approach, commonly adopted for ordinary buildings and deriving from the balance between the costs of repair and the social benefits associated with the implementation of a new infrastructure, may not be applicable to the case at hand in which the existing structures have an exceptional historical, monumental and artistic value. In this case it is necessary to adopt more stringent criteria to define acceptable thresholds, especially for very low, almost "cosmetic", levels of damage, but also to provide appropriate mitigation measures and criteria for their conditional activation.

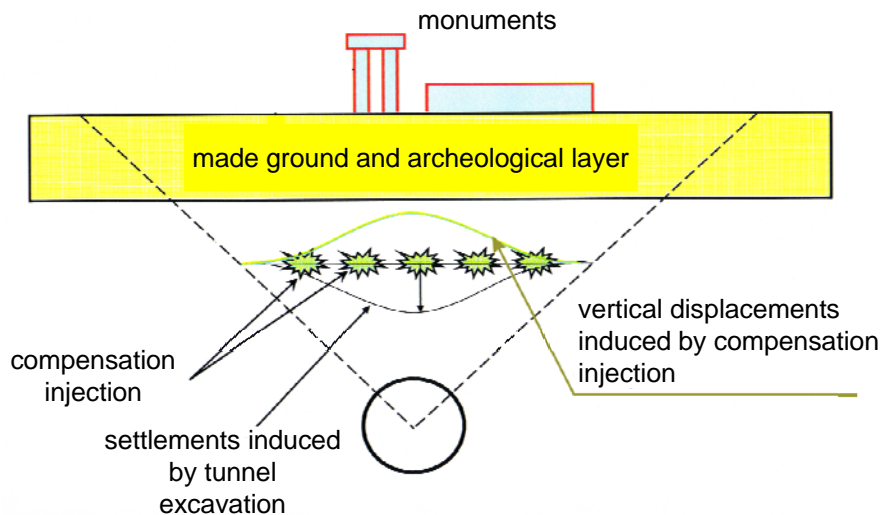


Fig. 8.2 – Schematic illustration of the compensation grouting technique.

Compensation grouting is a technique that is being increasingly used to control ground and building movements during tunnelling in soft ground. Figure 8.2 illustrates the principles of the method. During tunnelling, grout is injected from tubes installed in the soil between the tunnel and the building foundations (in this specific case, below the archaeological layer) to compensate for ground loss and stress relief caused by the tunnel excavation. The sleeved grout tubes (*tubes à manchette* or TAMs) are installed in the ground prior to tunnelling, often arranged radially from vertical shafts or from the surface by directional drilling. Installation of the TAMs can cause settlements, but these can be minimised by various means. Before tunnelling commences, conditioning grouting is undertaken to tighten the ground, fill any existing voids and reverse any settlement or loosening of the ground caused by drilling for TAM installation. Conditioning is usually achieved by injecting grout in a uniform density over a prescribed area until instrumentation installed on the ground surface or on overlying structures begins to respond, thus showing that the ground is fully tightened. Grout injection is then undertaken simultaneously with tunnelling in response to detailed observations, the aim being to limit building settlements and distortions to specified, acceptable amounts.

The importance of site coordination and high level site supervision of compensation grouting cannot be overemphasized. Properly conducted field trials prior to tunnelling are vital to prove the feasibility of TAM installation and the proposed grout mixes, and to validate assumptions regarding grout spread.



In addition to tunnelling, the construction of the deep open excavations required to accommodate the new stations may result in ground movements that can induce damage to adjacent buildings. If the excavation is supported by cast *in situ* reinforced concrete diaphragm walls, the displacements of the ground may result both from the installation of the panels by slurry trenching and concreting, and from the actual excavation in front of the diaphragm wall. Generally, to limit the horizontal displacements and hence the induced settlements of the buildings during excavation, stiff diaphragm walls and props installed as the excavation progresses are used. However, vertical stress relief associated to excavation induces surface settlements even when the retaining walls are prevented from moving horizontally, and deep-seated inward displacements of the walls that cannot be controlled by the props that are installed within the excavation itself. Therefore, to minimise the impact of deep excavations in urban areas, inward displacements of diaphragm walls and surface settlements around excavations may be reduced installing an internal support system below the formation level, prior to excavation.

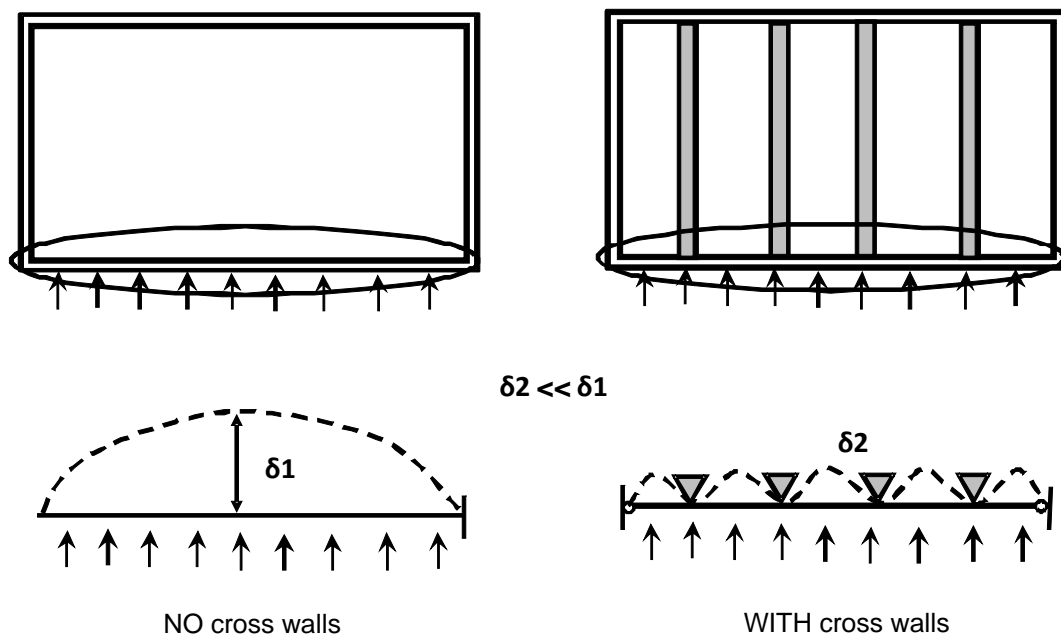


Fig. 8.3 – Principle of operation of sacrificial cross-walls

Sacrificial cross-walls may be formed by jet-grouted columns or unreinforced panels installed with diaphragm walling equipment. They are installed between the perimeter diaphragm walls before the start of excavation and are excavated out with the soil down to the depth of the final excavation level, see Figure 8.3. At the end of the excavation, the only portion of the cross-walls remaining to resist to the horizontal deflection of the diaphragm walls is that extending below the bottom of excavation. The need to demolish without too much difficulty sacrificial panels requires that they be designed seeking an effective compromise between their stiffness, necessary for the performance of their duty, and their strength, which should be low enough to make them easily excavated by ordinary equipment. Careful consideration is also required for the retaining wall design, to account for increased moments and shears.

## 9 CONCLUSIONS

Contracts T2 and T3 of the new line C of Rome underground underpass the historical centre of the city where masonry buildings of particular relevance are present, mostly built between the XV and the XIX centuries. A reliable evaluation of the potential damage induced by tunnel excavation to the existing building is essential in order to proceed with design, implementing where necessary appropriate mitigation techniques.

The procedure developed for evaluating these effects hinged on the geotechnical analyses, starting from a careful geotechnical characterisation based on *in situ* and laboratory tests and including the use of reliable computation models, but at the same time promoted a fruitful interaction of the geotechnical and structural engineers. At several stages, parallel evaluation of the damage to the buildings were carried out by both groups using the tunnelling-induced displacement fields computed in the geotechnical analyses. These independent estimates by the geotechnical and the structural engineers always provided consistent results.

Evaluation of tunnelling-induced effects was carried out following procedures of increasing level of complexity. Level 1 green-field evaluations were carried out using empirical relationships and assuming that the buildings follow the ground displacements; in some cases, at a subsequent stage, depending on the results of Level 1 analyses and on the specific relevance of the building, Level 2 interaction analyses were carried out in which the influence of the weight and the stiffness of the building was explicitly considered using a simplified description of the building through an equivalent solid entirely embedded into the soil, down to the foundation level. In addition to the study of the soil-structure interaction, these numerical analyses permitted to evaluate the long-term settlements that may develop when tunnels are excavated in fine-grained soils of very low permeability.

As a general result, explicit consideration of stiffness and weight of the building resulted in somewhat larger settlements but smaller distortions, and therefore predicted a lower damage if compared with the green-field. The reduction in the curvature of long-term settlement troughs resulted in a reduction of the predicted damage to the buildings.

In the evaluation of the potential damage it is very important to assess the magnitude of the background noise, *i.e.* of the movements of buildings due to external causes, such as daily and seasonal temperature cycles, fluctuations in the water level of the Tiber river, as it provides the reference lower bound of acceptable movements.

Finally, accurate monitoring and provision of measures for the protection of the monuments from the effects of the construction are two key aspects of the whole process that can be effectively implemented only if they are included consistently as part of the observational method in geotechnical design.

## 10 ACKNOWLEDGMENTS

The Authors are grateful to the Grantor, Roma Metropolitan SrL, and the General Contractor, Metro C SpA, for making this unique geotechnical experience possible. Special thanks are also due to the other members of the Technical and Scientific Steering Committee, and particularly to profs. Jamiolkowski, Carbonara, Kovari, and Macchi. The Authors also remember fondly the late prof. Funicello, who died in 2009, leaving a huge void in the Committee.

## 11 REFERENCES

BOSCARDIN M.D., CORDING E.J. (1989). Building response to excavation – induced settlement, *Journal of Geotechnical Engineering*, ASCE, vol. 115 (1), 1 – 21

BURLAND J.B. (1995). Assessment of risk of damage to buildings due to tunneling and excavation, *1st Int. Conf. on Earthquake Geotechnical Engineering*, Tokyo, 1189 – 1201

BURLAND J.B., BROMS B.B., De MELLO V.F.B. (1977). Behaviour of foundations and structures – SOA report, *9th Int. Conf. on Soil Mechanics and Foundations Engineering*, Tokyo, vol. 2, 495 – 546

BURLAND J.B., Wroth C.P. (1974). Settlement of buildings and associated damage, *Proc. Conf. Settlement of Structures*, Cambridge, UK, 611 – 654

CALABRESI, G., CASSINIS, C. e NISIO, P. (1980) – Influenza del regime del Tevere sul comportamento di un fabbricato monumentale adiacente. *XIV Convegno Nazionale di Geotecnica*. Firenze

FINNO, R. J., VOSS JR. F. T., ROSSOW, E. & BLACKBURN, J. T. (2005) – Evaluating Damage Potential in Building Affected by Excavations. *Journal of Geotechnical and Environmental Engineering*, ASCE, Vol. 131, No 10, October, 1119-2100.

MAIR R.J., TAYLOR R.N., BRACEGIRDLE A. (1993). Subsurface settlement profiles above tunnels in clay, *Geotechnique*, vol. 43 (2), 315 – 320

MAIR, R. J. & TAYLOR, R. N. (1997) – Bored tunneling in the urban environment. State-of-the-art report and theme lecture. Proc. 14<sup>th</sup> Int. Conf. Soil Mech. Found. Engng, Hambourg 4, 2353-2385

MAIR, R. J. (2008) -46<sup>th</sup> Rankine Lecture. Tunnelling and geotechnics: new horizons. *Géotechnique* 58, No 9, pp. 695-736

MAZARS, J. (1984) – Application de la mécanique de l'endommagement au comportement non linéaire et à la rupture du béton de structure. Thèse de Doctorat d'Etat, L.M.T., Université Paris, France.

MOH Z.C., HWANG R.N., JU D.H. (1996). Ground movements around tunnels in soft ground, Proc. Int. Symp. on Geotechnical Aspects of Underground Construction in Soft Ground, London, 725 – 730

O'REILLY M.P., NEW B.M. (1982). Settlements above tunnels in the United Kingdom – Their magnitudes and prediction, Proc. Tunnelling '82 Symp., London, 173 – 181

PECK, R. B. (1969) – Deep excavations and tunnelling in soft ground. State of the art report, Mexico City, *State of the Art Volume*. Proc. 7th Int. Conf. SMFE, pp. 225-290.

PICKHAVER, J. A. (2006)- Numerical Modelling of Building Response to Tunnelling. PhD Thesis. University of Oxford

RANKIN, W. J. (1988) – Ground movements resulting from urban tunneling; predictions and effects. Engineering Geology of Underground Movement, Geological Society. Engineering Geology Special Publication No 5, pp. 79-92.

RIBACCHI R. (1993). Recenti orientamenti nella progettazione statica delle gallerie, XVIII Convegno Nazionale di Geotecnica, Rimini, vol. 2, 37 – 92

SCHANZ T., VERMEER P.A., BONNIER P.G. (1999). Formulation and verification of the Hardening – Soil Model. Proceedings Plaxis Symposium "Beyond 2000 in Computational Geotechnics", Amsterdam, 18 – 20 March 1999, 281 – 296

SCHMIDT B. (1969). Settlements and round movements associated with tunnelling in soil, Ph.D. Thesis, University of Illinois, 224 pp.

VOSS, F. (2003) - Evaluating Damage Potential in Building Affected by Excavations. MS thesis, Northwestern University Evanston, IL. 166 p.

WONGSAROJ, J. (2005) – Three-dimensional finite elements analysis of short- and long-term ground response to open face tunneling in stiff clay. PhD Thesis, Cambridge University.